

7355

MSFC
MTP-RP-61-17/
October 3, 1961
Cp 3

68 85057
Code 5

GEORGE C. MARSHALL SPACE FLIGHT CENTER

53P 13 ref

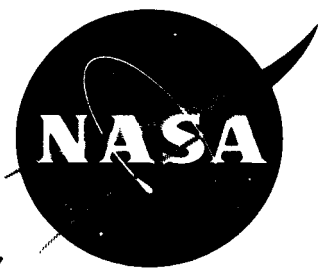
HUNTSVILLE, ALABAMA

(NASA TM 450428)

TEMPERATURE CONTROL OF THE S-15 PAYLOAD
(EXPLORER XI)

By
William C. Snoddy

PROPERTY OF
TECHNICAL DOCUMENTS
UNIT, NASA-IPL



FOR INTERNAL USE ONLY



RQT-7355

GEORGE C. MARSHALL SPACE FLIGHT CENTER

MTP-RP-61-17

TEMPERATURE CONTROL OF THE S-15 PAYLOAD
(EXPLORER XI)

by

William C. Snoddy

ABSTRACT

This report deals with the thermal design of the S-15 payload (Explorer XI, Gamma Ray Astronomy Satellite) placed into orbit by the 19E Juno II vehicle on April 27, 1961. The discussions include: (1) need for thermal design, (2) approach used, (3) theoretical model, (4) design tests, and (5) comparison of actual in-orbit data with theoretical data.

GEORGE C. MARSHALL SPACE FLIGHT CENTER

MTP-RP-61-17

TEMPERATURE CONTROL OF THE S-15 PAYLOAD
(EXPLORER XI)

by

William C. Snoddy

SPACE THERMODYNAMICS BRANCH
RESEARCH PROJECTS DIVISION

ACKNOWLEDGMENTS

The author wishes to acknowledge extensive work which has been done on the thermal control of this payload by several others:

Mr. R. B. Merrill set up the theoretical temperature equation and carried out the analytical design study.

Mr. Cliff Lumpkin and Miss Betty Bobo helped in the reduction and analysis of the satellite data.

Mrs. Billy Robertson programmed and ran the theoretical equations on the IBM 7090 computer.

TABLE OF CONTENTS

	Page
SECTION I. Introduction	1
SECTION II. Thermal Design Philosophy	11
SECTION III. Theoretical Calculations	14
SECTION IV. Thermal Testing	15
SECTION V. Results	32
SECTION VI. Results of Special Temperature Measurements . .	38

LIST OF ILLUSTRATIONS

Figure	Title	
1.	Gamma Ray Astronomy Satellite (S-15)	2
2.	Artist's Sketch of S-15 Satellite	3
3.	Marshall Instrument Package	4
4.	MIT Instrument Package	5
5.	Artist's Sketch of the S-15 Payload	7
6.	Payload Attached to Fourth Stage Rocket	8
7.	Mercury Damper	9
8.	Mercury Damper Attached to Fourth Stage Rocket . . .	10
9.	Internal View of Solar Cell "Box"	12
10.	Vacuum Chamber	17
11.	Cut-Away of "Full Blanket" Test Set-Up	18
12.	Calibration Sphere Showing One of the Thermocouples	19

LIST OF ILLUSTRATIONS (Cont'd)

Figure	Title	Page
13.	Calibration Sphere in Chamber	20
14.	Heater Blanket Inside Calibration Sphere	21
15.	Theoretical and Measured Temperature of Radiation Heat Sink Test	22
16.	Full-Blanket on Prototype	26
17.	Half-Blanket on Prototype	27
18.	Half-Blanket Covered by Foil Reflector	28
19.	Digital Data Recorder	29
20.	Results from Full-Blanket Test.	30
21.	Results from Half-Blanket Test	31
22.	Juno II Vehicle	33
23.	Temperature of Motor Case Versus Minutes after Egress from Earth's Shadow	34
24.	Theoretical Solar Attitude Versus Days after Launch	35
25.	Average Value of Motor Case Temperature During First 15 Minutes after Satellite Emerges from Earth's Shadow Versus Days after Launch	36
26.	Percent Time of Satellite's Orbit in Sunlight	37
27.	Temperature of Thermally Isolated Sensor Versus Days after Launch	39
28.	Temperature of Solar Cell Patches Versus Minutes from Egress and Pass Number	40
29.	Temperatures of MIT and Marshall Packages Versus Days after Launch	41

LIST OF ILLUSTRATIONS (Cont'd)

Figure	Title	Page
30.	Thermally Isolated Temperature Sensor	42
31.	Temperature of Thermally Isolated Temperature Sensor Versus Minutes after Egress from Earth's Shadow	44

GEORGE C. MARSHALL SPACE FLIGHT CENTER

MTP-RP-61-17

TEMPERATURE CONTROL OF THE S-15 PAYLOAD
(EXPLORER XI)

by

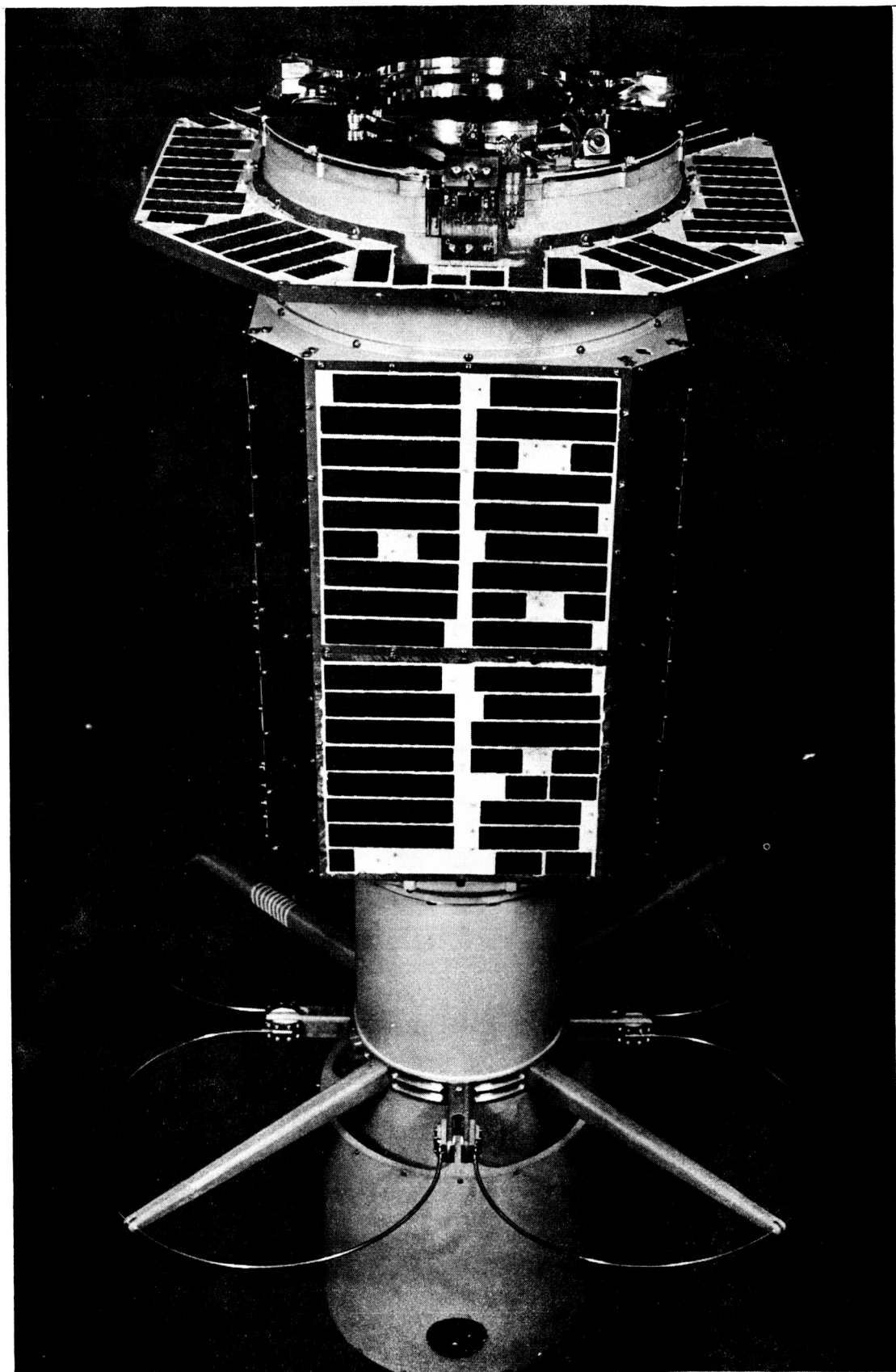
William C. Snoddy

SUMMARY

This report deals with the thermal design of the S-15 payload (Explorer XI, Gamma Ray Astronomy Satellite) placed into orbit by the 19E Juno II vehicle on April 27, 1961. The discussions include: (1) need for thermal design, (2) approach used, (3) theoretical model, (4) design tests, and (5) comparison of actual in-orbit data with theoretical data.

SECTION I. INTRODUCTION

The NASA S-15 payload (Explorer XI) is known as the Gamma Ray Telescope Satellite (FIG. 1 and 2) and has as its major objective the detection and measurement of energetic cosmic gamma radiation in the 100 mev region (1). It was constructed, assembled, and tested by the Marshall Space Flight Center (FIG. 3); the experiment package was built and supplied by the Massachusetts Institute of Technology (FIG. 4). The payload was placed in orbit on April 27, 1961 using the Juno II (19E) vehicle (2). Initially, it had an apogee of 1799.08 km; perigee of 490.81 km; inclination of 28.80 degrees; and a period of 108.12 minutes. The satellite is powered by solar cells and can be commanded on and off by ground stations. It is planned, however, to operate the payload at least one year before it is commanded off. When the payload was first placed in orbit, it was spinning at approximately 400 rpm about its longitudinal axis. Since this is an unstable axis, the payload gradually "opened up" into a flat "propeller-like" spin or tumble about an axis perpendicular to the original spin axis, with the spin about the longitudinal axis going to zero. If angular momentum was conserved, the ratio of the rate of spin about the final axis to the rate about the initial axis was the same as the inverse of the ratio of the moments of inertia about the respective axes (3). The change of spin mode was noted for Explorers I, III, and IV (4) which had the same type of mechanical configuration as the S-15 payload.



MTP-RP-61-17

FIGURE 1. GAMMA RAY ASTRONOMY SATELLITE (S-15)

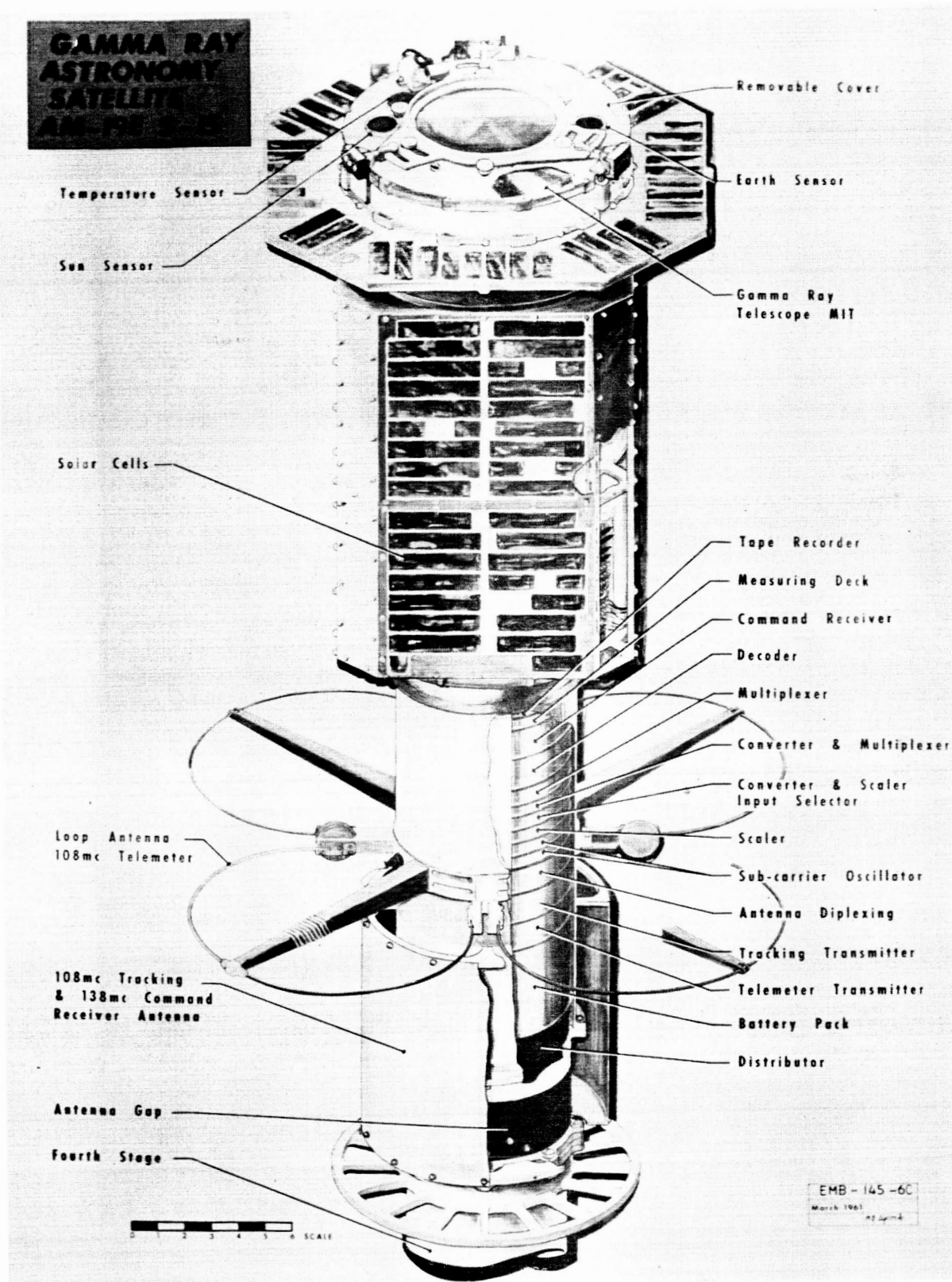
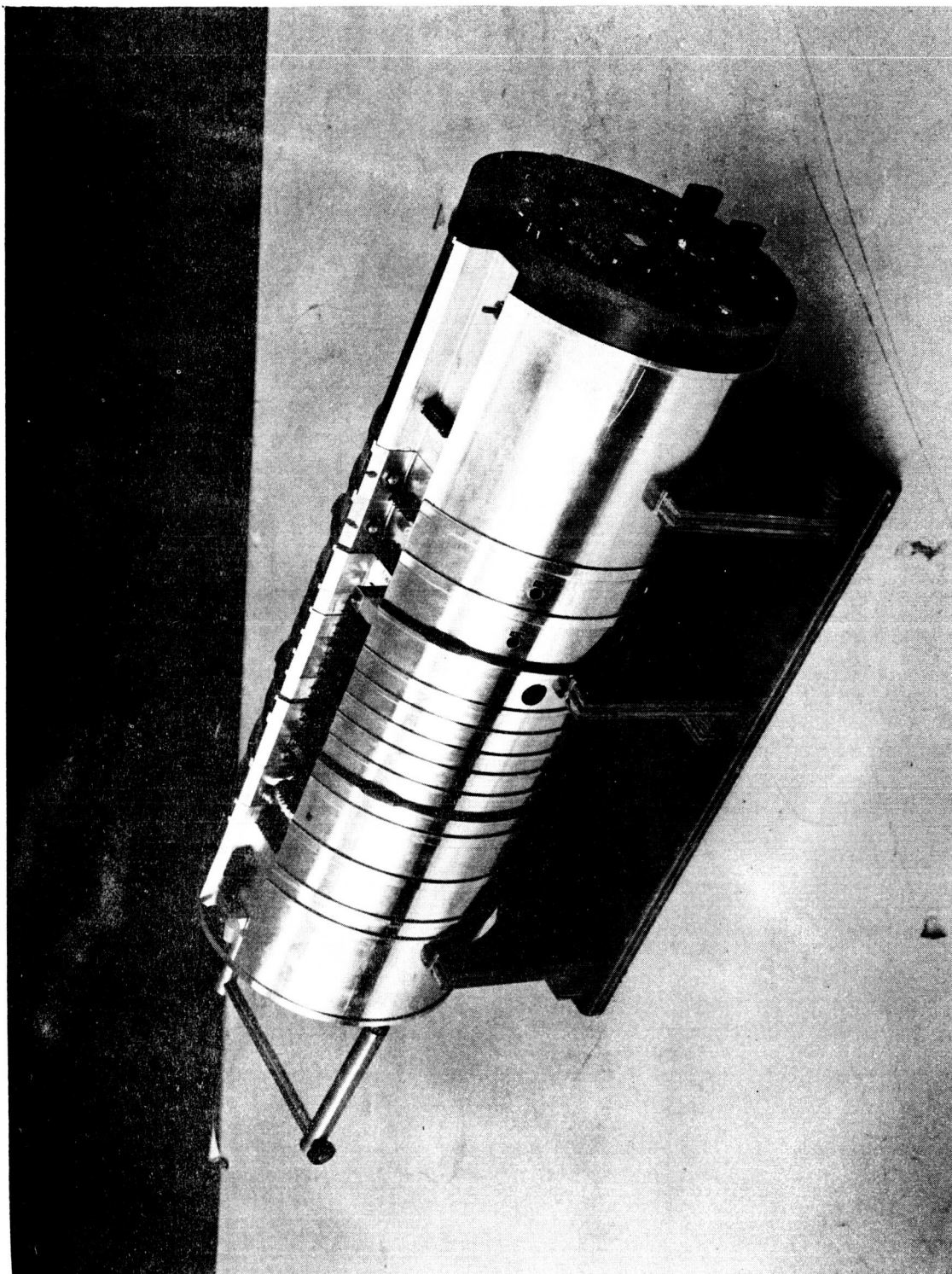


FIGURE 2. ARTIST'S SKETCH OF S-15 SATELLITE MTP-RP-61-17



MTP-RP-61-17

FIGURE 3. MARSHALL INSTRUMENT PACKAGE

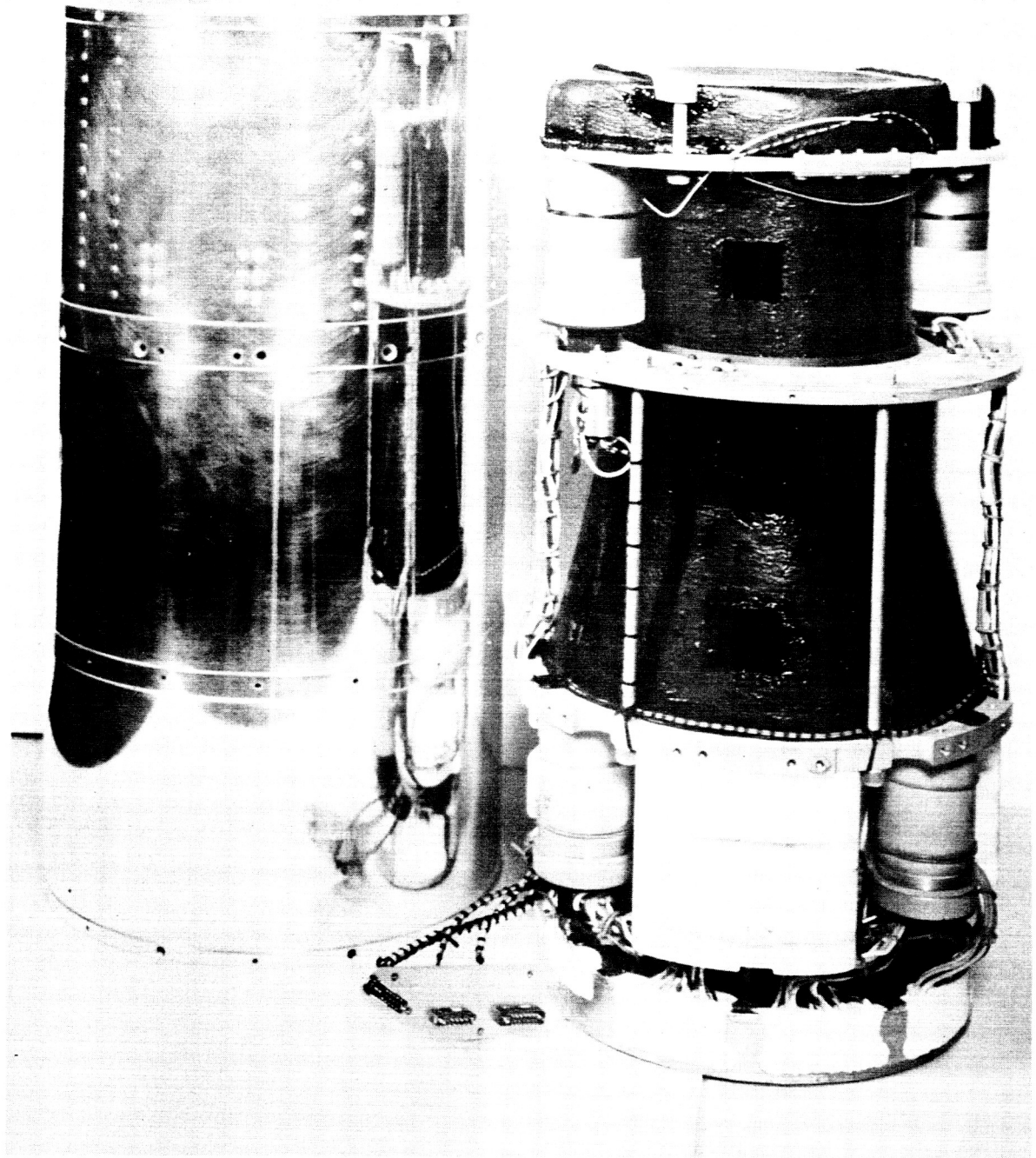


FIGURE 4. MIT INSTRUMENT PACKAGE

MTP-RP-61-17

This configuration was purposely chosen for S-15 so that the gamma ray telescope could "look" out of the end of the satellite and scan a great circle on the celestial sphere each time the payload tumbled (FIG. 5). In order to facilitate this conversion from initial spin mode to the final tumble mode, the fourth stage rocket was left attached to the payload, rendering the initial spin axis even more unstable (FIG. 6). In addition, a special double-walled stainless steel cylinder with liquid mercury between the walls was attached to the fourth stage rocket (FIG. 7 and 8). The purpose of the mercury was to help dissipate the energy which must be lost as the payload changes modes of spin and thus decrease the length of time required for the change. The mercury also damped out any nutations which occurred after this final tumble situation was reached (3).

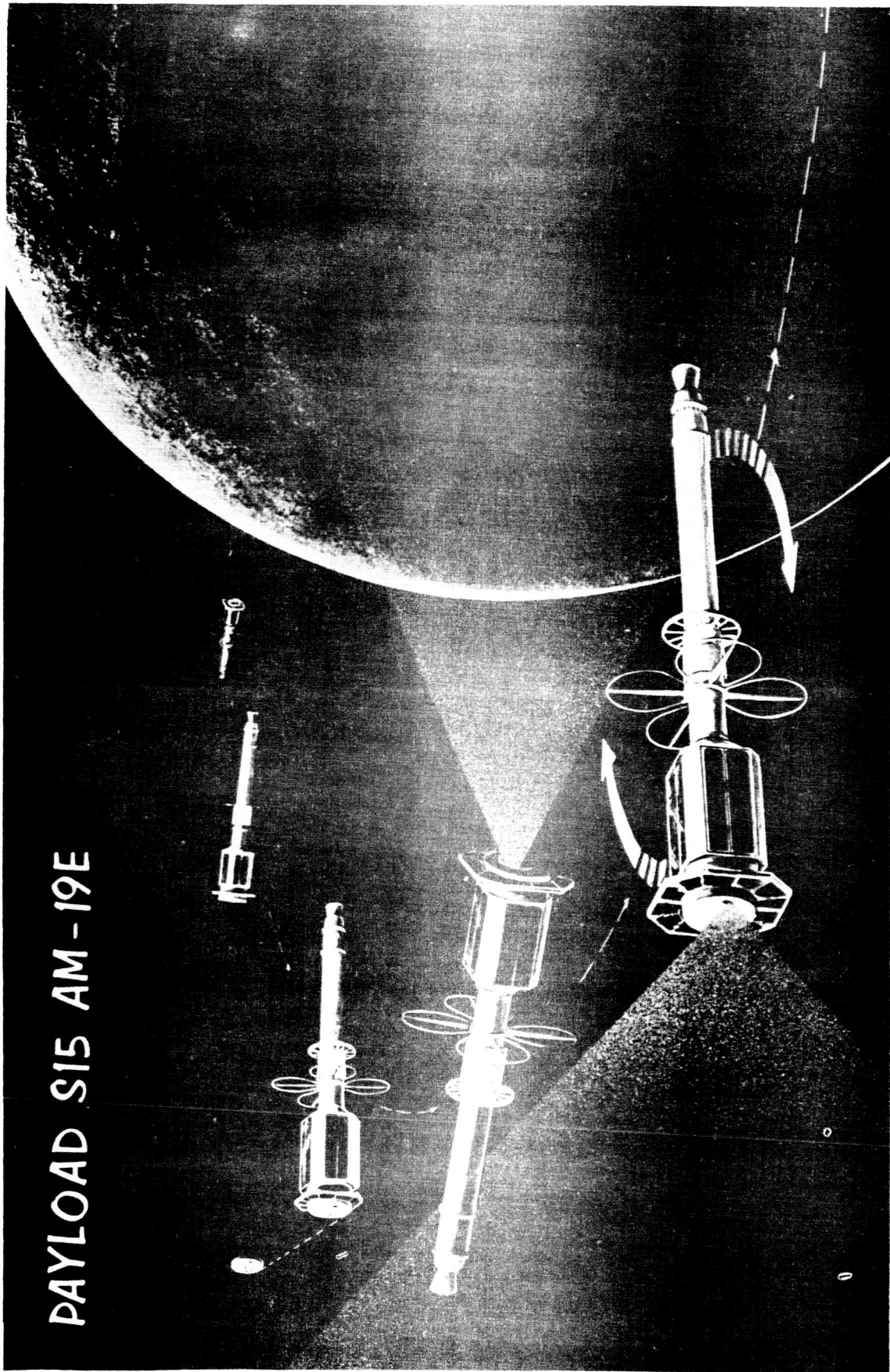
The need for temperature control of this payload arose from the thermal sensitivity of the instrumentation and batteries. The payload was designed such that the temperature of these components would remain within the range of 0° to 60° C.

The temperature of an object in a vacuum, such as space, is determined by the radiation exchange with its environment and any internal energy conversion to or from heat. In the case of a near-earth satellite, the major radiation environment is made up of direct solar radiation, reflected solar radiation from the earth, earth infrared radiation, and reflected and infrared radiation from the satellite. Thus far, internal energy conversion to or from heat in most satellites has been limited to ohmic heat generation.

The amount of heat entering a satellite varies throughout a revolution as the payload passes through the earth's shadow, changes altitude and earth-fixed attitude, and varies in angular distance from the subsolar point on the earth. A much slower effect on heat input occurs with changes in the plane of the orbit with respect to the sun and the earth, the argument of perigee, the percent of the orbit in sunlight, and the solar attitude of the payload. The amount of heat leaving the payload varies solely as the fourth power of the temperature of the radiating surface. This is under the assumption that there are no changes in the amount or surface characteristics of the external area.

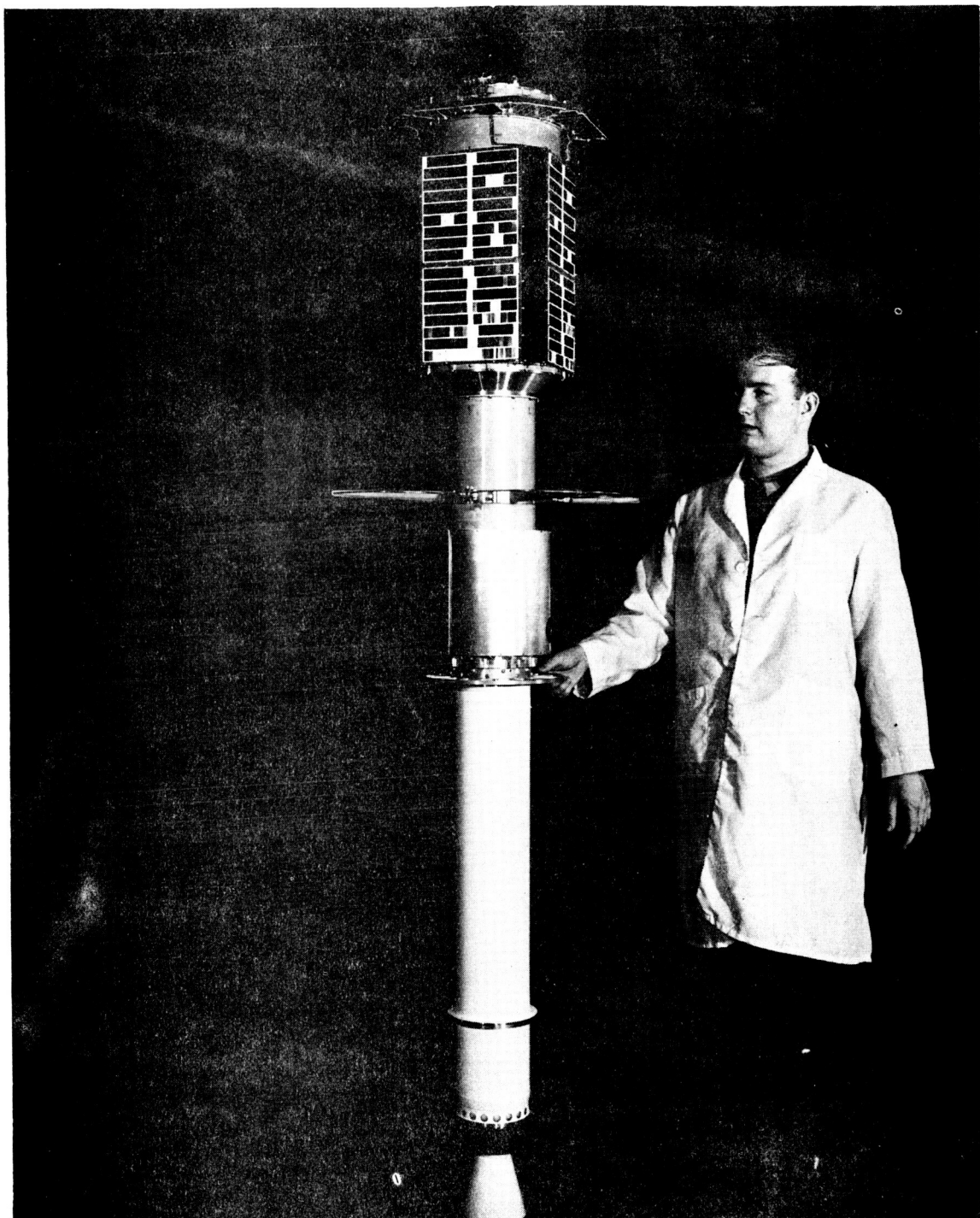
The internal heat generation for the S-15 payload was less than 1 watt. Almost all of this heat was produced in the area of the transmitter and caused only a few degrees rise in the temperature of the nearby instrumentation.

PAYLOAD S15 AM-19E



MTP-RP-61-1

FIGURE 5. ARTIST'S SKETCH OF THE S-15 PAYLOAD



MTP-RP-61-17
FIGURE 6. PAYLOAD ATTACHED TO FOURTH STAGE ROCKET

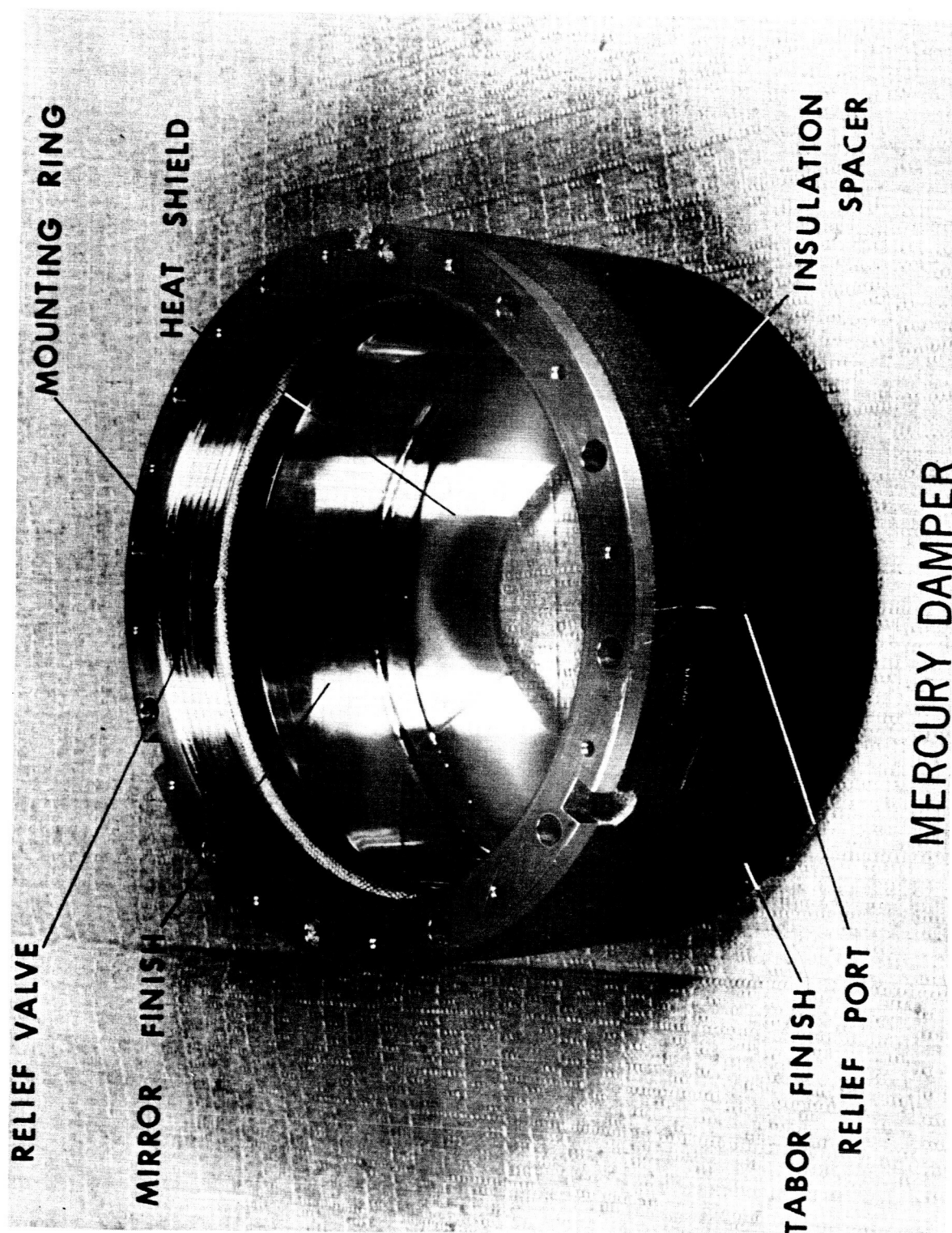
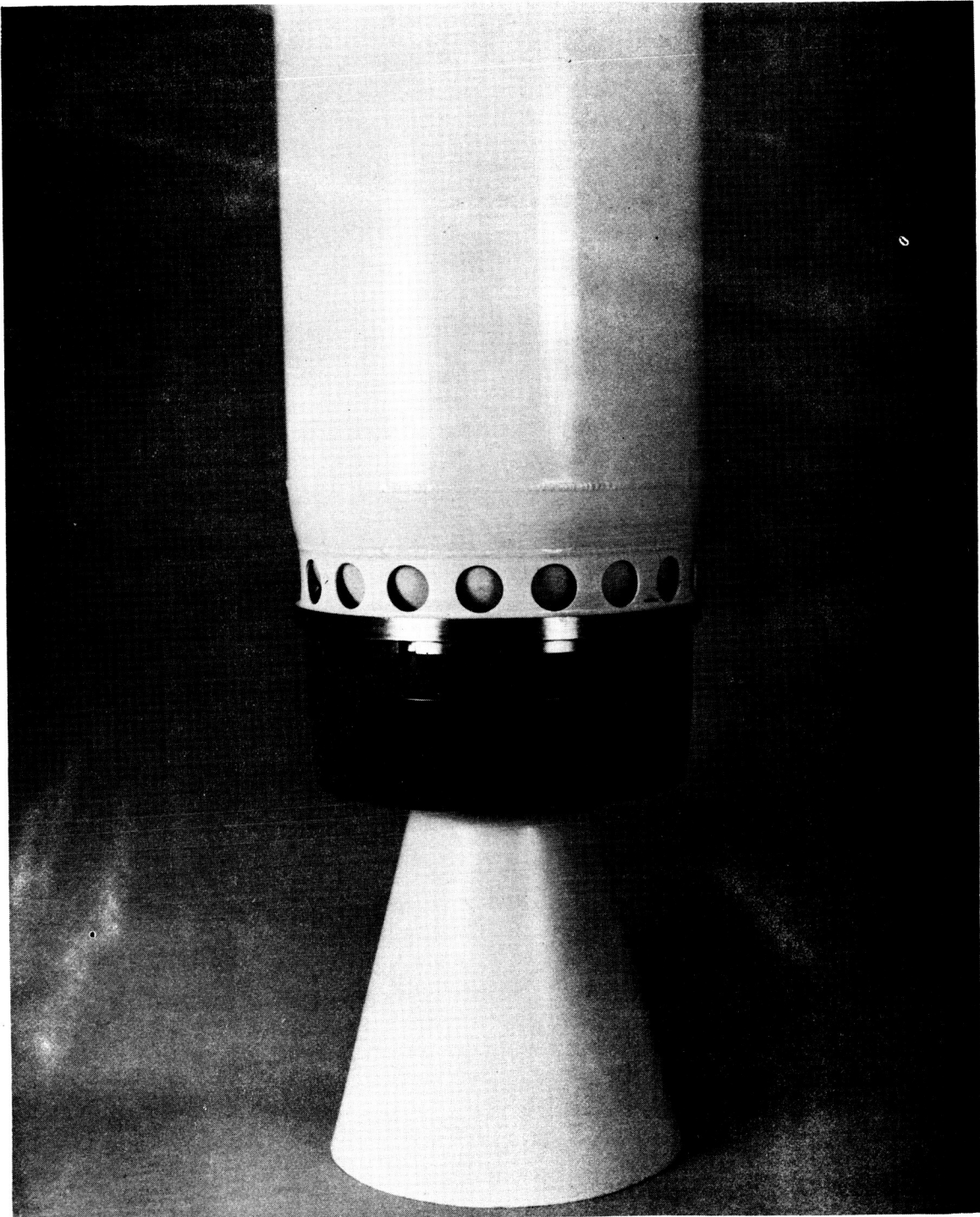


FIGURE 7. MERCURY DAMPER



MTP-RP-61-17

FIGURE 8. MERCURY DAMPER ATTACHED TO FOURTH STAGE ROCKET

SECTION II. THERMAL DESIGN PHILOSOPHY

Preliminary studies determined that the passive methods of temperature control used on earlier Explorer satellites would suffice for this payload (5-10). This is, while the temperature of the skin of the payload fluctuated widely during a revolution as the net amount of heat entering the payload changed, the time-average temperature was controlled by proper selection of the radiative characteristics of the surfaces. The temperature fluctuations were damped out from the thermally sensitive components by the use of thermal insulation. The temperature-sensitive components were located in either the MSFC instrument package or the MIT package. Both packages were mounted on Kel-F or fiberglass spacers to reduce conduction transfer to the skin and were highly polished to prevent radiation. All parts of the satellite which could "see" either of these packages were also polished to reduce radiation transfer. Thermal insulation is especially important in this type of payload because of the possibility of occasions when large temperature gradients ($\Delta T \approx 100^\circ\text{C}$) will exist around the longitudinal axis of the payload. These gradients are caused when the attitude of the satellite, with respect to the sun, is such that the sun is perpendicular to the plane of flat spin. If the spin rate about the longitudinal axis reaches zero, the sun would radiate on just one side of the payload causing a large gradient. With sufficient insulation, however, the thermal linkage between the sensitive components and the skin can be made much smaller than the thermal transfer within the components, allowing the components to be fairly isothermal regardless of the large gradients existing around the skin.

Although the insulation damps out most of the fluctuations during one revolution, it is not sufficient to damp out the variations in the average value of the skin temperature over a period of several days. Consequently, there is a slow day-to-day variation in the temperature of the sensitive components.

The proper radiating characteristics of the external surfaces were obtained by analytical juggling of the various surface finishes until the desired over-all combination was obtained. The various surfaces included: solar cells, cement containing a white paint, anodized magnesium, sandblasted aluminum, polished aluminum, black paint, and a special "Tabor" - type finish (TABLE I).

In addition to the external surface treatment and the thermal insulation of the sensitive components, other steps were taken in the thermal design of S-15. All areas which could radiate to each other in the cavity between the solar cell plates and the outside of the shell cylinder containing the MIT package were painted with a high emissivity white paint (FIG. 9).

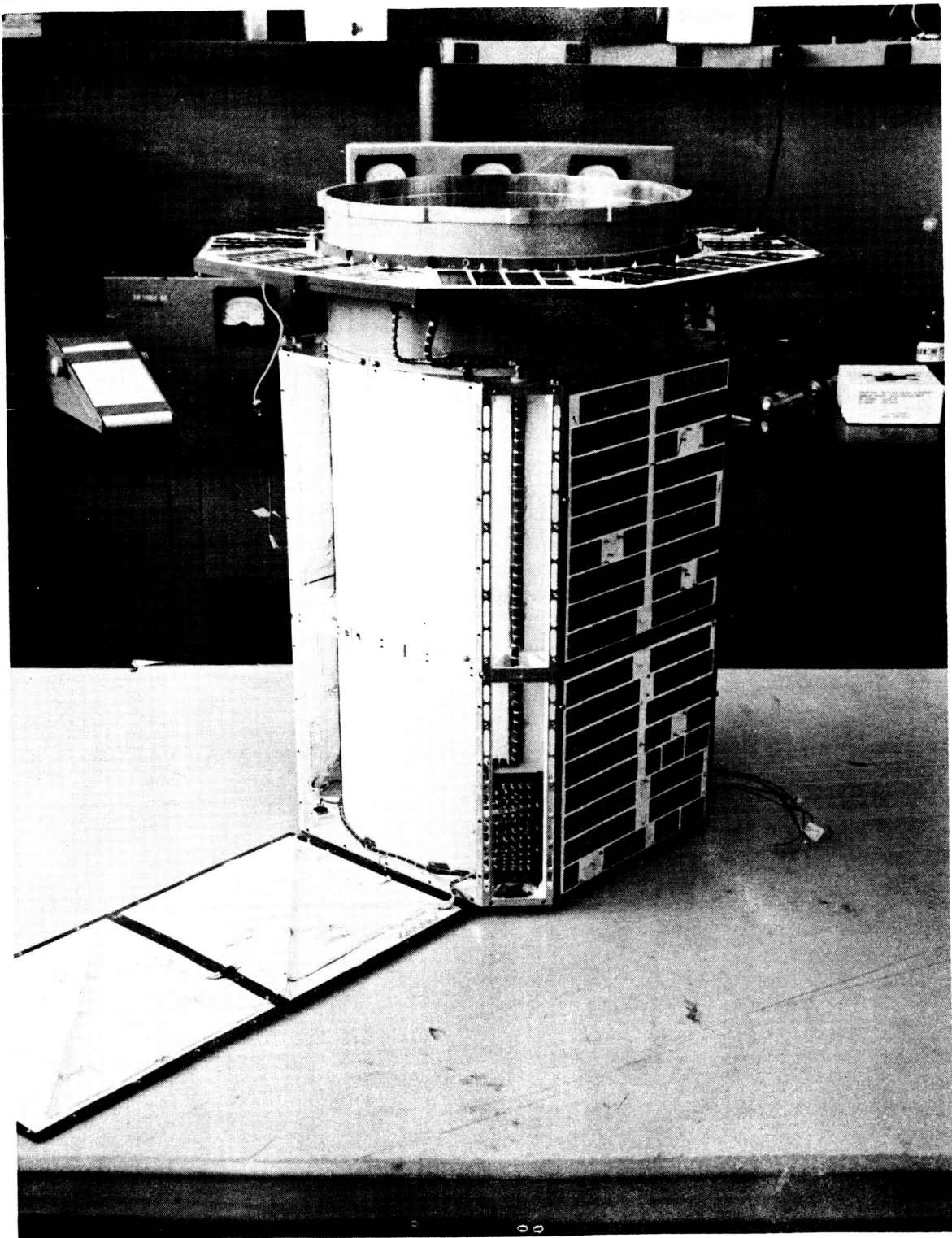


FIGURE 9. INTERNAL VIEW OF SOLAR CELL "BOX" MTP-RP-61-17

This was done in order to facilitate the equalization of the skin temperature. For the same reason, the inside of the 108 and 138 mc antenna cylinder was painted with the high emissivity paint, as well as the outside of the shell cylinder underneath the antenna can. A thin Kel-F spacer was placed between the points of contact of the antenna cylinder and the fourth stage to aid in thermally insulating the motor case from the rest of the payload.

TABLE I
EXTERNAL SURFACE FINISHES

AREA	α	ϵ
Solar Cell Plates		
Solar cells	0.80	0.40
Anodized magnesium	0.88	0.93
Cement	0.30	0.80
Heat Balance Strips		
"Tabor" surface	0.9	0.4
Top Plate		
Polished aluminum	0.2	0.08
Mercury Damper		
"Tabor" surface	0.9	0.4
Motor Case		
White paint between shell loop antenna can	0.25	0.8
Black paint	0.95	0.90
All Other Major Areas		
Sandblasted aluminum	0.51	0.32

SECTION III. THEORETICAL CALCULATIONS

Two theoretical temperature programs were set up on the IBM 7090 computer as an analytical aid in completing the thermal design of the payload (11). In both programs, the satellite was broken up into sections which were assumed to be isothermal. In the first program, it was assumed that the satellite had sufficient spin about its longitudinal axis to equalize the temperatures about this axis and, consequentially, only thirteen sections were chosen. In the second program, it was assumed that the spin about the longitudinal axis was zero, and twenty-two sections were used. In both programs, a heat balance equation of the following form was written for each section:

$$\begin{aligned} \dot{T}_i H_i = & A_{1i} \alpha_i S D_1 + A_{2i} \alpha_i B S g D_2 + A_{3i} \epsilon_i E S g \\ & - A_{4i} \epsilon_i \sigma T_i^4 + \sum_j \left[R_{ij} (T_j^4 - T_i^4) + C_{ij} (T_j - T_i) \right] \\ & + Q_i \end{aligned}$$

where

T_i = temperature of area "i"

H_i = heat capacity

A_{1i} = effective area to solar radiation

α_i = solar absorptivity

S = solar radiation flux

D_1 = 1 when satellite is in sunlight, 0 when in shadow

A_{2i} = effective area to earth albedo

B = ratio of earth albedo flux to solar radiation flux

g = altitude factor

D_2 = factor based on angular distance of satellite from subsolar point on earth

- A_{3i} = effective area to earth infrared radiation
 E = ratio of earth infrared flux to solar radiation flux
 A_{4i} = radiating area
 σ = Boltzmann constant
 R_{ij} = radiation constant between areas "i" and "j"
 C_{ij} = conduction constant between areas "i" and "j"
 T_j = temperature of area "j"
 Q_i = internal heat generation
 ϵ = infrared emissivity

This group of nonlinear differential equations was then numerically solved throughout the complete orbit. By using the computer program, the external surfaces and internal insulation could be determined. The program is also used in evaluating the temperature data recorded from 8 thermistors on the satellite, and the data obtained during thermal testing.

SECTION IV. THERMAL TESTING

A prototype of the payload was subjected to two types of thermal tests in order to check the various thermal transfer coefficients and thermal time constants. One test consisted of cooling the prototype to a uniform temperature of about -20°C . Then, while in a vacuum of 5×10^{-4} mm Hg, or better, the outside surfaces were raised to a temperature of 70°C and the temperatures of various parts of the instrument package were recorded. From these tests, it was possible to get the over-all thermal transfer coefficients between various parts of the instrument package and the skin.

In the second set of tests, an actual orbital situation was simulated. As discussed earlier, when the payload is in orbit, it is designed to go into a flat propeller-like tumble with the spin around the longitudinal axis decreasing to zero. Therefore, a "worst" situation was simulated in which the sun would "see" the payload at an angle perpendicular to the plane of flat spin and in which the position of the longitudinal orientation was such that the sun was also perpendicular to one side of the solar cell box. This is a situation in which the largest temperature gradients around the longitudinal axis should occur.

With a vacuum pulled and the payload at ambient temperature, heat was applied to those areas that the sun would "see" at this solar attitude angle. By use of the theoretical temperature computer program, calculations were made to determine the net amount of heat to apply to these surfaces as a function of their temperatures. As the surface temperatures increased, the heat inputs were decreased to the point that the heat entering the surfaces no longer increased the surface temperatures and was conducted and radiated to the unheated parts of the prototype which were allowed to radiate freely. Thus, a steady state condition, very close to that in space previously described, was established. Gradients were obtained between various parts of the satellite, and with a knowledge of the heat input, the thermal transfer coefficients were determined.

The tests were conducted in the same manner as those for S-1, S-46, S-30, and S-45 payloads (12, 8, 9, 10). The test requirements were specified to the Electro-Mechanical Branch of Guidance and Control Division and made a part of the test specifications. A detailed procedure was set up by the E-M Branch using the same method of blanket heating and liquid nitrogen cooling as used in the earlier thermal tests.

The vacuum requirement was met by running the tests in a large chamber (located in the S&M Division) capable of attaining a pressure of about 3×10^{-7} mm Hg (FIG. 10). The payload was initially cooled by running liquid nitrogen into a special double-walled liner which had been built into the vacuum chamber (FIG. 11). The liner covered all walls of the chamber and half of the door; the other half was covered with aluminum foil. In the orbital simulation test (half-blanket test) this liner was used to simulate the perfect radiation heat sink of space. The liner was filled with liquid nitrogen and radiated very little heat to the payload. By coating its inside surface with a special black carbon paint, the heat radiated from the payload was almost entirely absorbed. A test was conducted to determine how well this combination of low temperature and high absorptivity simulated a perfect radiation heat sink. A sphere was coated with a paint of known emissivity (FIG. 12 and 13) and suspended inside the vacuum chamber. After a vacuum had been pulled and the liner filled with liquid nitrogen, the sphere was heated by means of a blanket placed inside it (FIG. 14). By monitoring the current and voltage, a given amount of power was fed into the blanket. It was assumed that upon reaching a steady state condition, all of the electrical power was converted into heat and radiated from the sphere. If one knows the amount to be radiated, the radiating area of the sphere, and the emissivity of the area, it is possible to calculate the temperature of the sphere's surface if it were radiating to a perfect radiation heat sink. These theoretical values are shown along with the actual measured values in FIGURE 15. As can be seen, the liner is a very good radiation heat sink and for the thermal testing is assumed to be perfect.

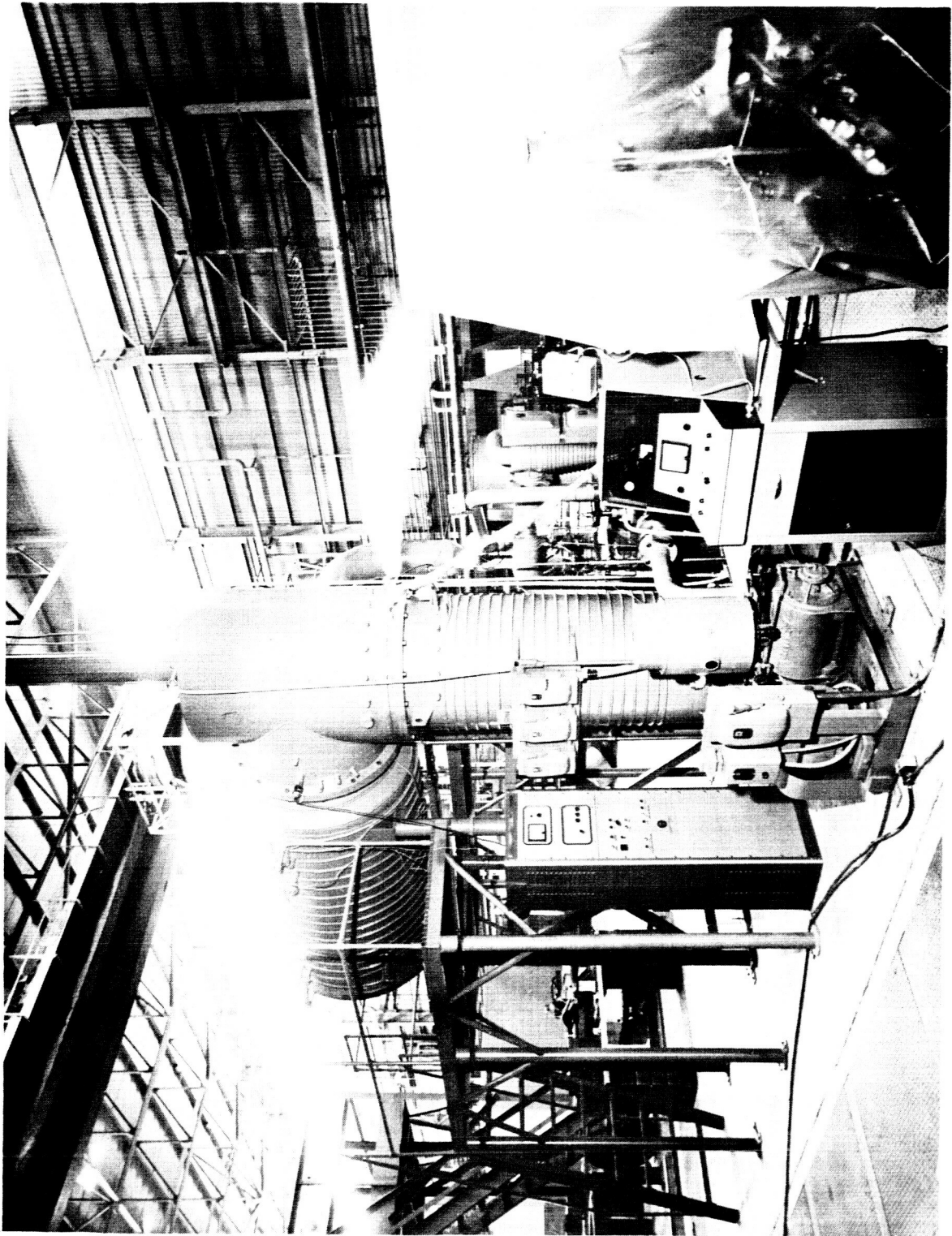
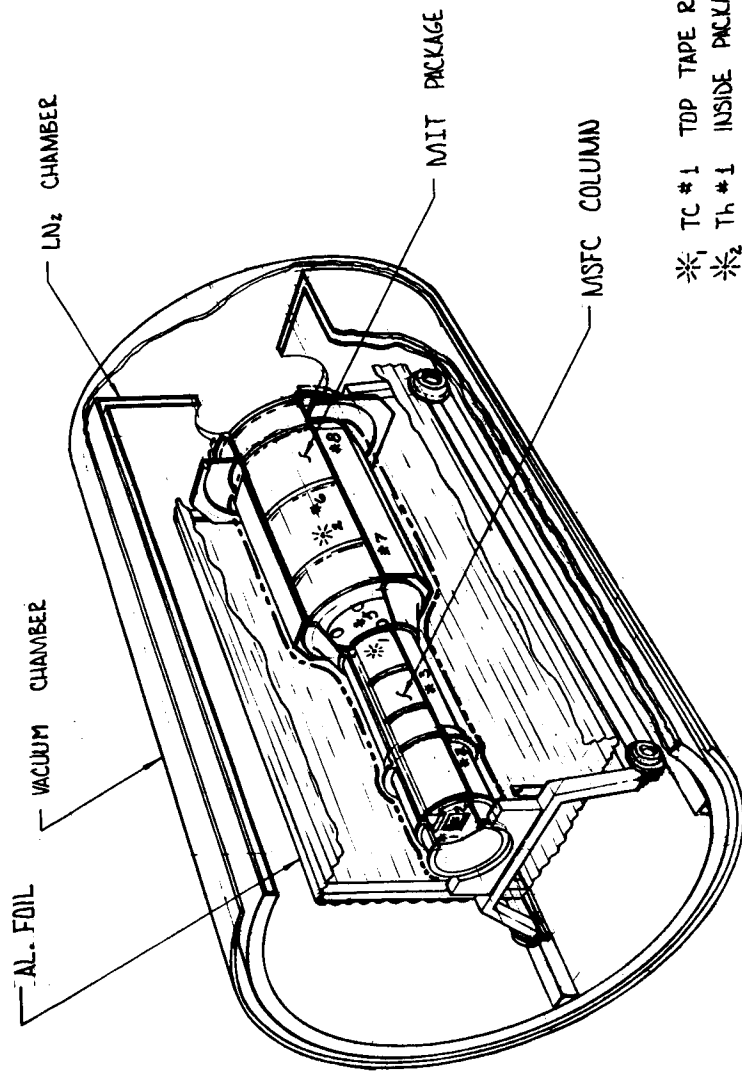


FIGURE 10. VACUUM CHAMBER



*₁ TC #1 TOP TAPE RECORDER

*₂ Th #1 INSIDE PACKAGE

*₃ TC #3 SHOWS RADIAL LOCATION, .5" DEEP

2 TC #4 ACTUAL LOCATION

3 TC #9+10 SHOWS RELATIVE LOCATION, INSIDE

4 TC #11+12 "

5 TC #8 ACTUAL LOCATION

6 TC #6+7 RELATIVE LOCATION

7 TC #15+16 RELATIVE LOCATION, INSIDE

8 TC #13+14 "

MTP-RP-61-17

FIGURE 11. CUT-AWAY OF "FULL BLANKET" TEST SET-UP

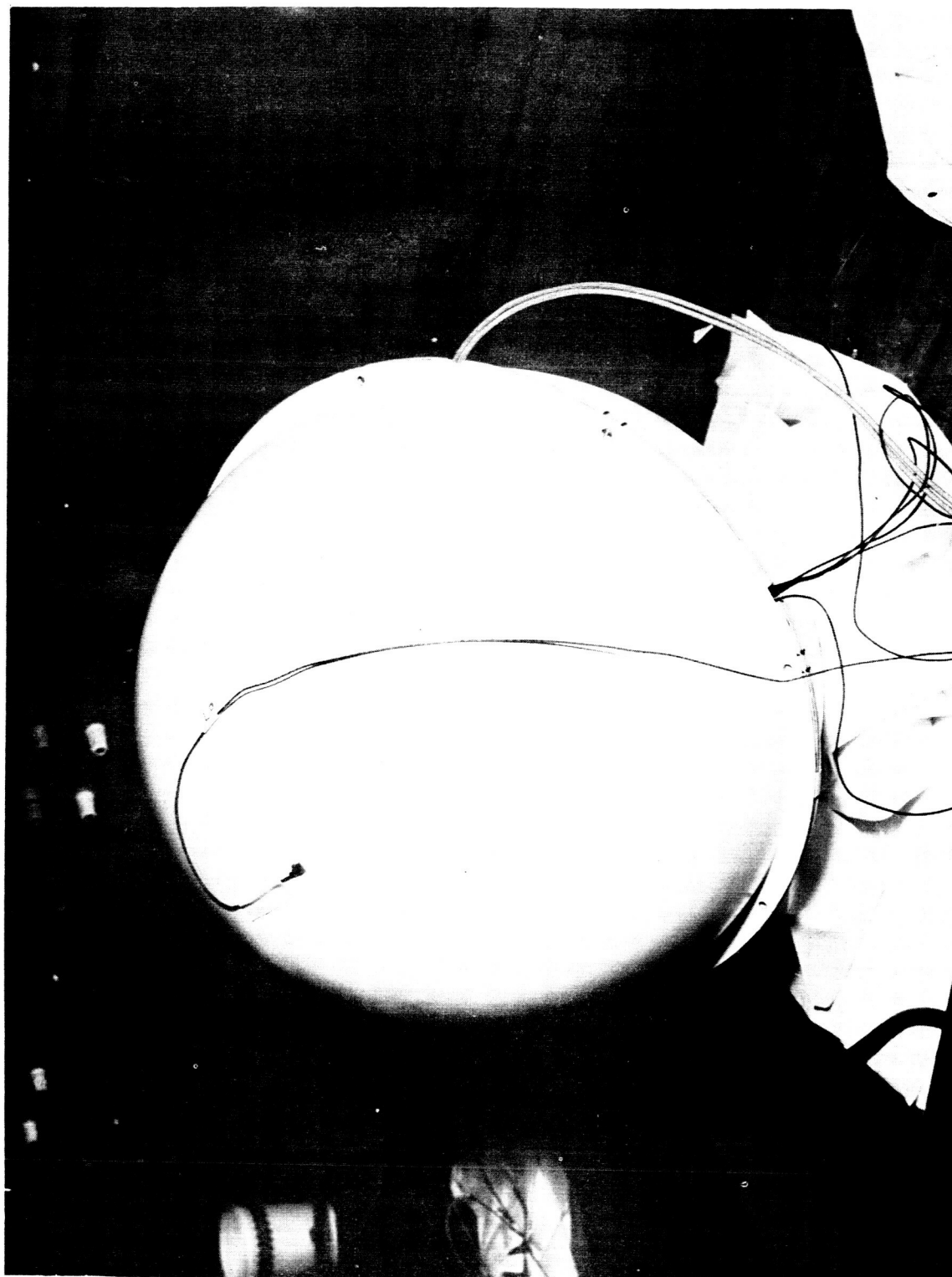


FIGURE 12. CALIBRATION SPHERE SHOWING ONE OF THE THERMOCOUPLES

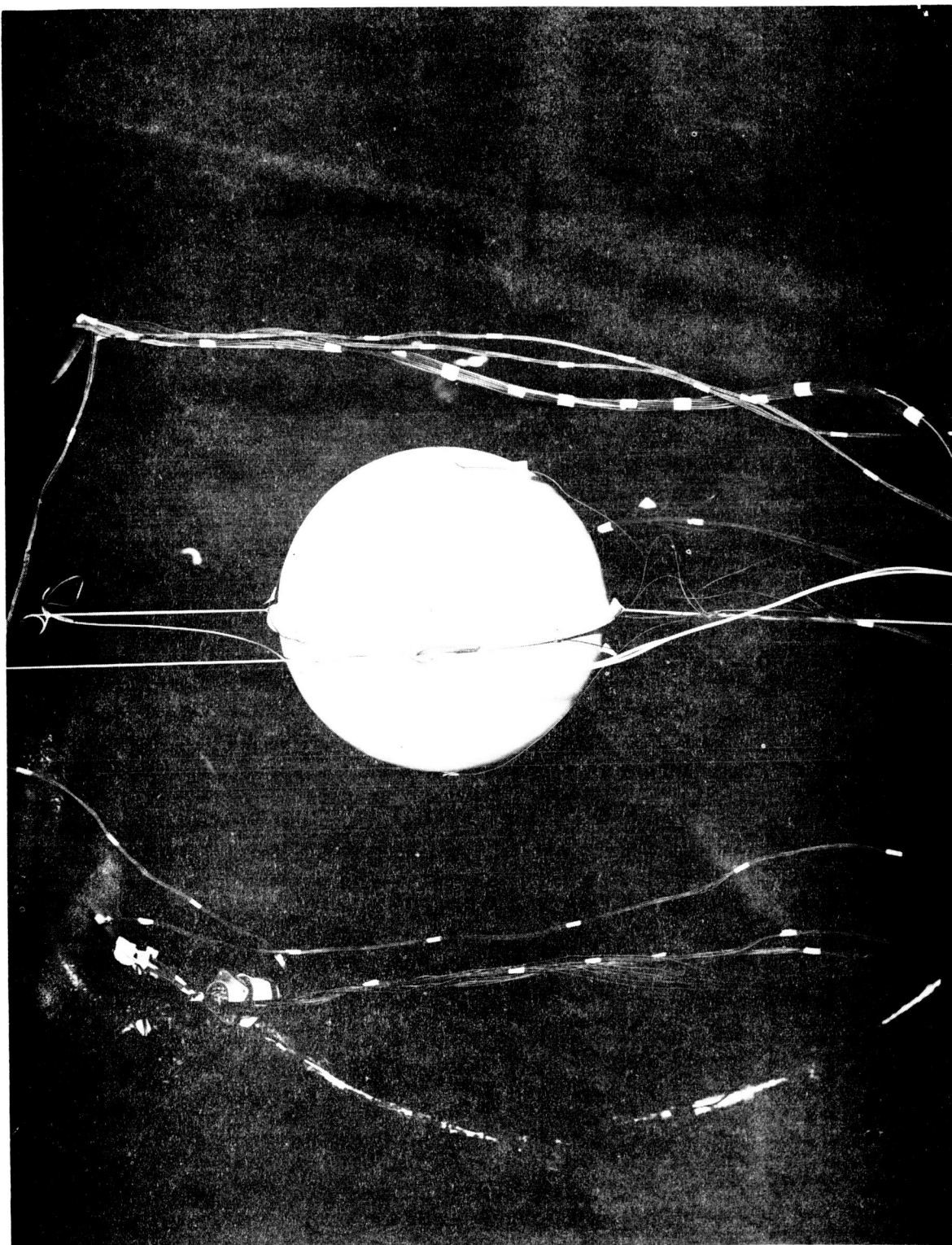
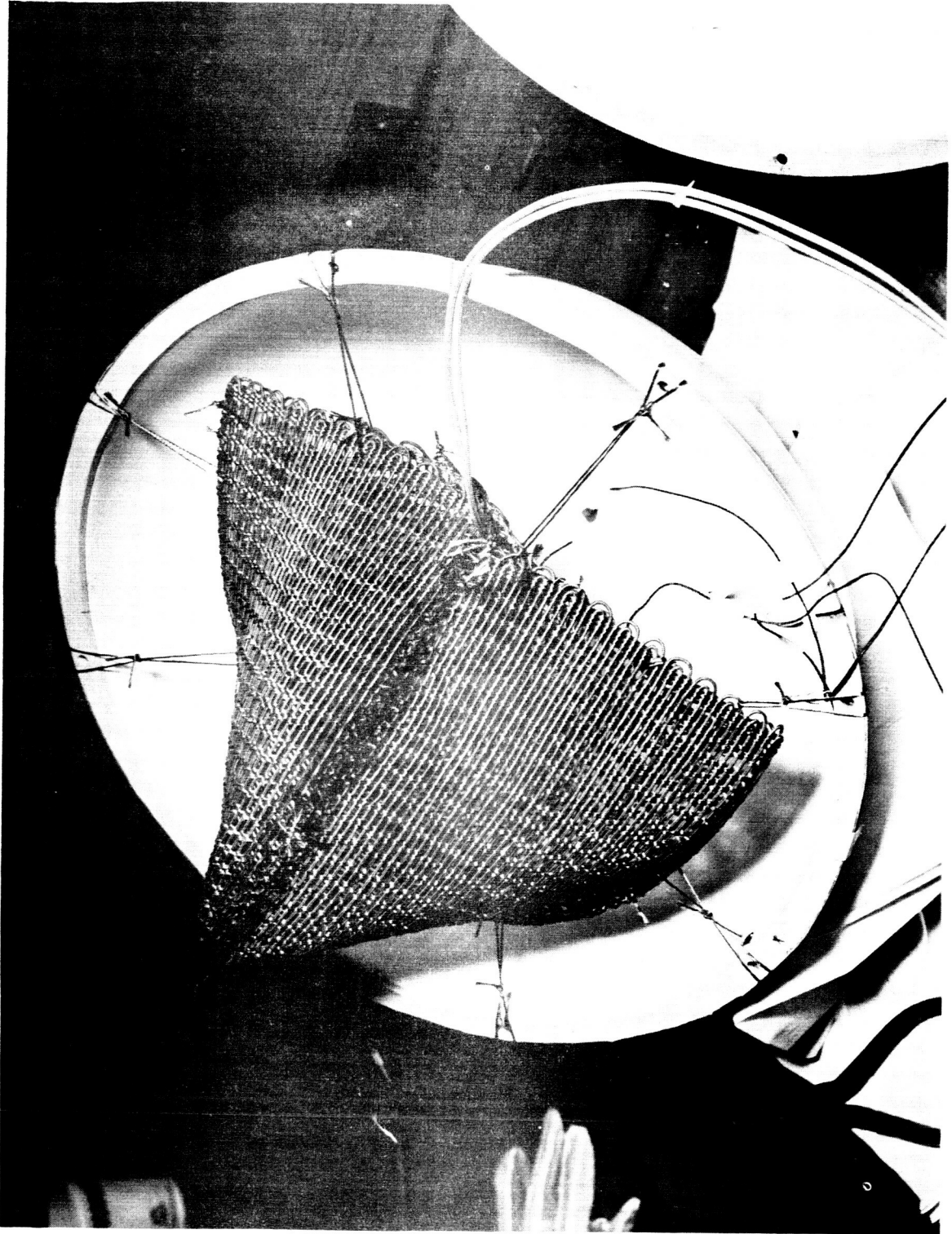
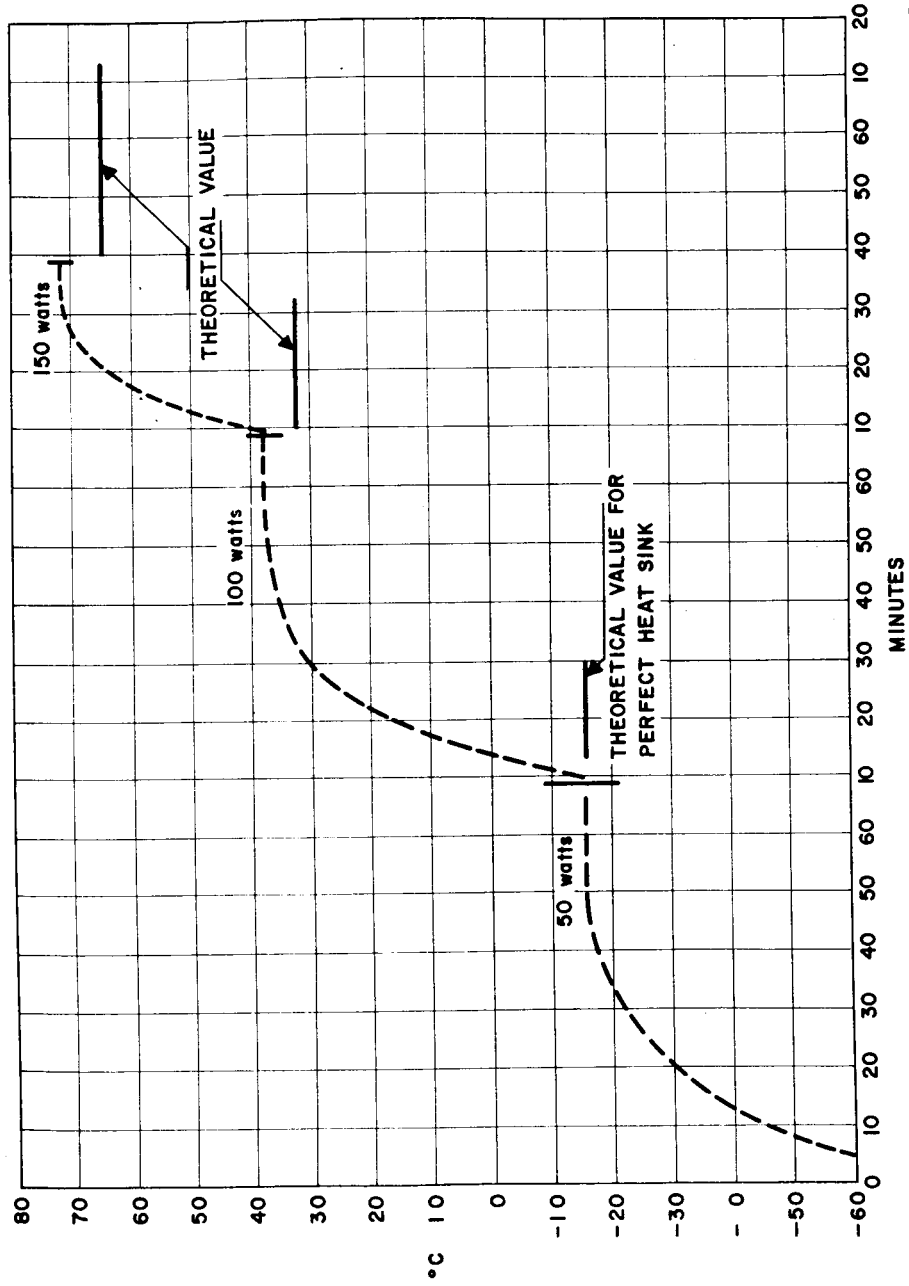


FIGURE 13. CALIBRATION SPHERE IN CHAMBER



MTP-RP-61-17

FIGURE 14. HEATER BLANKET INSIDE CALIBRATION SPHERE



MTP-RP-61-17

FIGURE 15. THEORETICAL AND MEASURED TEMPERATURE OF RADIATION HEAT SINK TEST

Cooling was accomplished with the aid of convection by filling the vacuum chamber with dry nitrogen. When the temperatures equalized at about -20°C , the dry nitrogen was pumped out and the heat applied using specially designed fitted blankets (FIG. 16 and 17). During the orbital simulation tests, the actual heat input was controlled by monitoring the blanket current and using foil reflectors (FIG. 18). During these tests, up to 46 thermocouples and 4 thermistors were attached to the payload, heater blankets, and heat sink to record their temperatures. Using a stepping switch, the thermocouple readings were digitally recorded (FIG. 19) in the control room where the controls of the blanket circuits were located. The locations of the thermocouples and thermistors are in TABLE II.

Some of the results from a "full blanket" test where heat was applied to all external surfaces are given in FIGURE 20. The sharp rise in temperature imposed on the shell of the prototype is shown by the curves labeled TC-10, 25. The insulation of the Marshall package (TC-2) and the MIT package (TH-1) is evident by their slow response to the increase in temperature. As can be seen, the time constants (time for gradient to decrease by one-half) for the Marshall and MIT packages are about 8 to 16 hours (extrapolating), respectively.

Some of the results of the orbital simulation test ("half-blanket") are shown in FIGURE 21. At time $t = 0$, a vacuum had already been pulled and the payload was at ambient temperature. The process of filling the liner with liquid nitrogen was begun and at $t = 50$ minutes; the blankets were turned on. The near steady state condition reached after approximately five hours running time, indicates the amount of heat transfer across the payload. Despite the large gradients across the payload, it was found that, due to the insulation, there was only a relatively small gradient across the instrument packages.

Since blankets were used as the heat source instead of a type of solar radiation simulation, the solar absorptivity of the surfaces during these tests could not be checked. This was accomplished by making emissivity and reflectivity measurements on specially prepared samples.

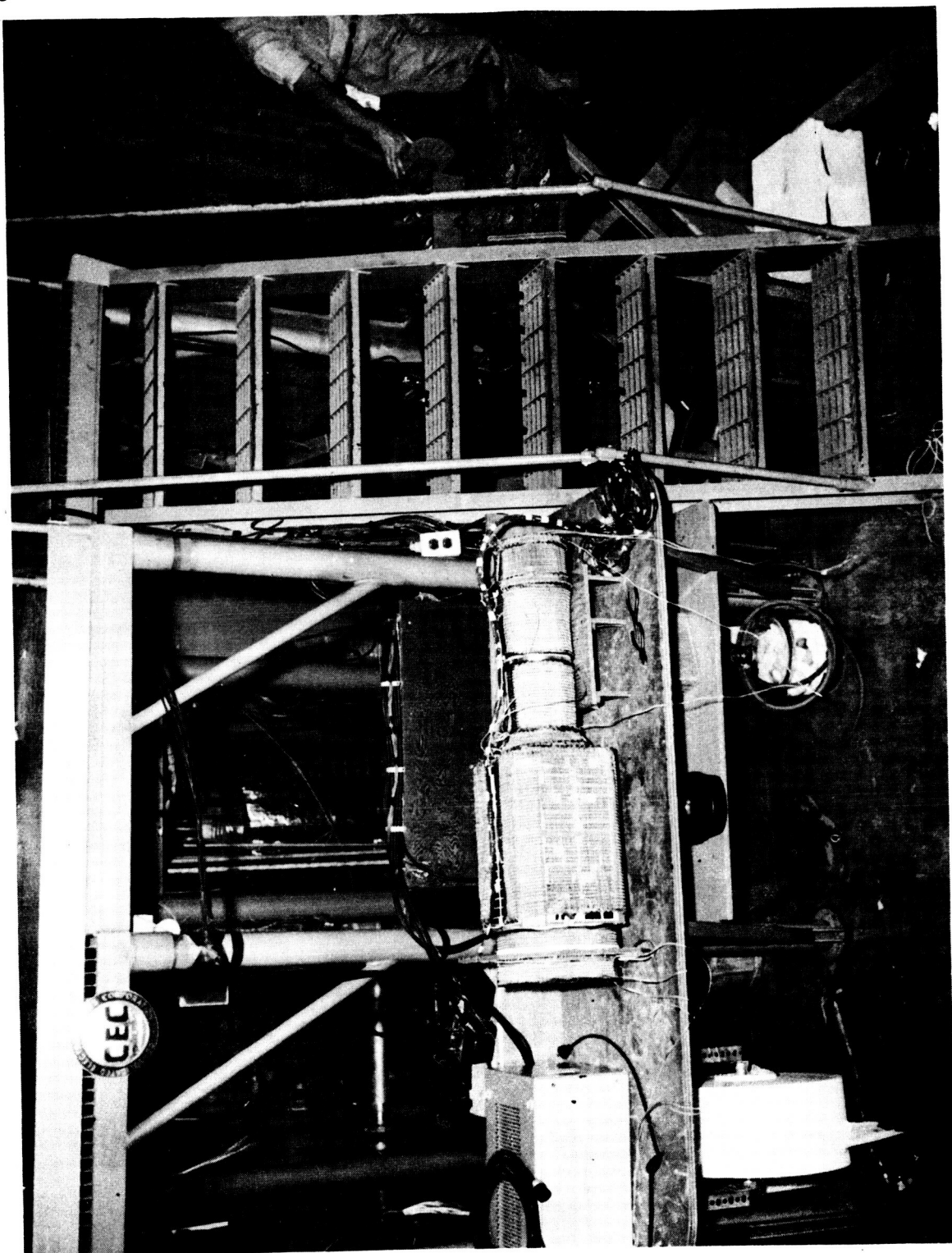
TABLE II
LOCATION OF THERMOCOUPLES

Thermocouple (No.)		Location (o'clock)
1	Top of Tape Recorder	
2	Tracking Transmitter Deck	
3	Inside Battery	
4	Bottom Distributor	
5	Top MIT Package (outside)	
6	Middle MIT Package (outside).	12:00
7	Middle MIT Package (outside).	6:00
8	Bottom MIT Package (outside)	
9	Near Top End Shell MSFC Pkg. (inside)	12:00
10	Near Top End Shell MSFC Pkg. (inside)	6:00
11	Near Bottom End Shell MSFC Pkg. (inside).	12:00
12	Near Bottom End Shell MSFC Pkg. (inside).	6:00
13	Near Top End Shell MIT Pkg. (inside).	12:00
14	Near Top End Shell MIT Pkg. (inside).	6:00
15	Near Bottom End Shell MIT Pkg. (inside)	12:00
16	Near Bottom End Shell MIT Pkg. (inside)	6:00
17	Near Bottom End Solar Cell Box (outside).	12:00
18	Near Bottom End Solar Cell Box (outside).	3:00
19	Near Bottom End Solar Cell Box (outside).	6:00
20	Near Bottom End Solar Cell Box (outside).	9:00
21	Near Bottom End Solar Cell Box.	12:00
22	Near Bottom End Solar Cell Box.	3:00
23	Near Bottom End Solar Cell Box.	6:00
24	Near Bottom End Solar Cell Box.	9:00
25	Heat Balance Strip (inside)	1:30
26	Heat Balance Strip (inside)	4:30
27	Heat Balance Strip (inside)	7:30
28	Heat Balance Strip (inside)	10:30
29	Base of Tabor Sensor	
30	Transition Cone	12:00
31	Transition Cone	6:00
32	Antenna Gap	12:00
33	Antenna Gap	6:00
34	Solar Cell Disc	12:00
35	Solar Cell Disc	6:00
36	Removable Shield	
37	LN ₂ Heat Sink	

TABLE II (Cont'd)

Thermocouple (No.)	Location (o'clock)
38	LN ₂ Heat Sink
39	LN ₂ Heat Sink
40	LN ₂ Heat Sink
41	LN ₂ Heat Sink
42	Number 1 Heater Blanket (Full Blanket Test)
43	Number 2 Heater Blanket (Full Blanket Test)
44	Number 3 Heater Blanket (Full Blanket Test)
45	Number 4 Heater Blanket (Full Blanket Test)
46	Number 5 Heater Blanket (Full Blanket Test)
42	Number 1A Heater Blanket (Half Blanket Test)
43	Number 2A Heater Blanket (Half Blanket Test)
44	Aluminum Foil Shield
45	Aluminum Foil Shield
46	Aluminum Foil Shield

Note: There were 4 thermistor measurements: 3 in the MIT package, and 1 on the special temperature sensor disc.



MTP-RP-61-17

FIGURE 16. FULL-BLANKET ON PROTOTYPE

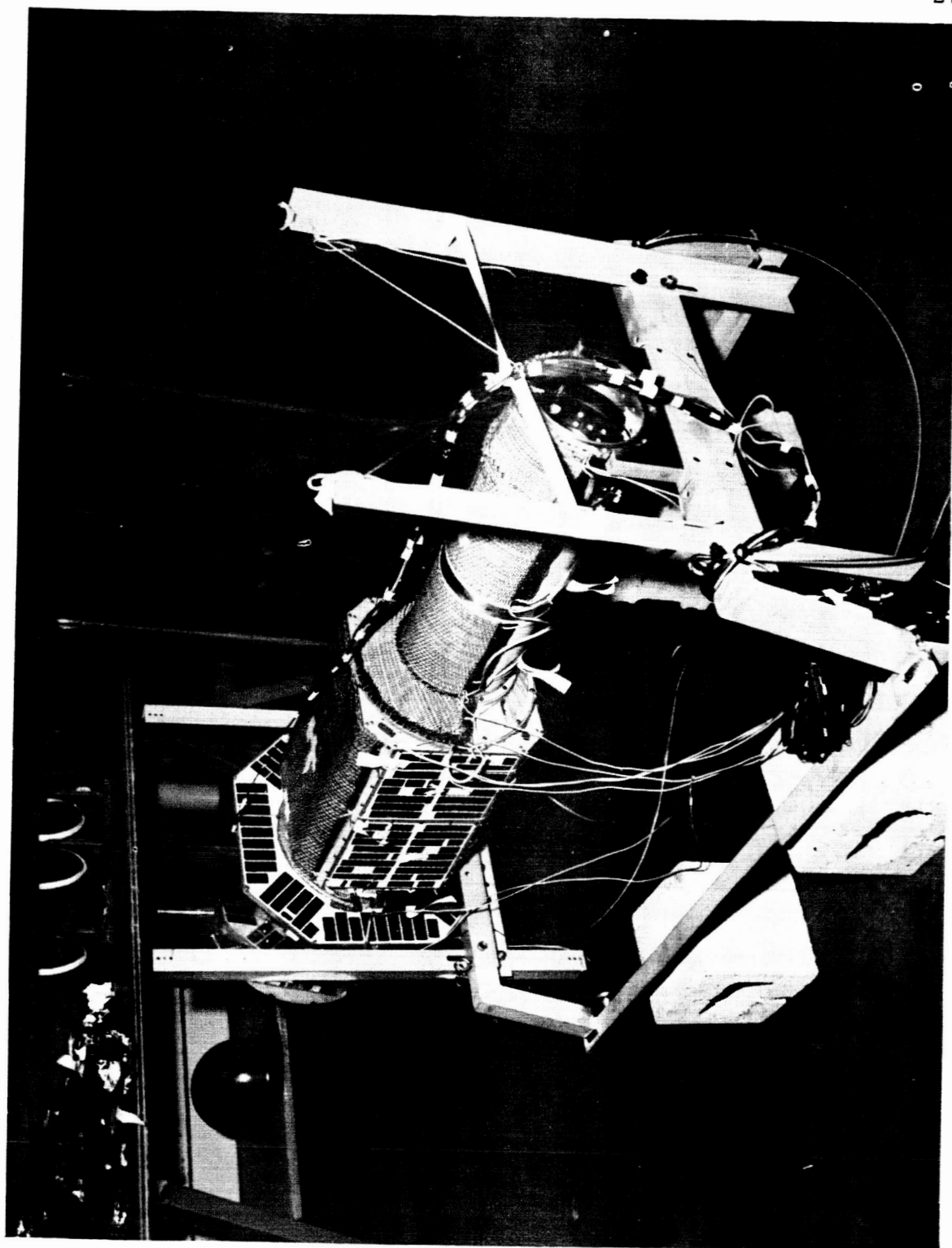
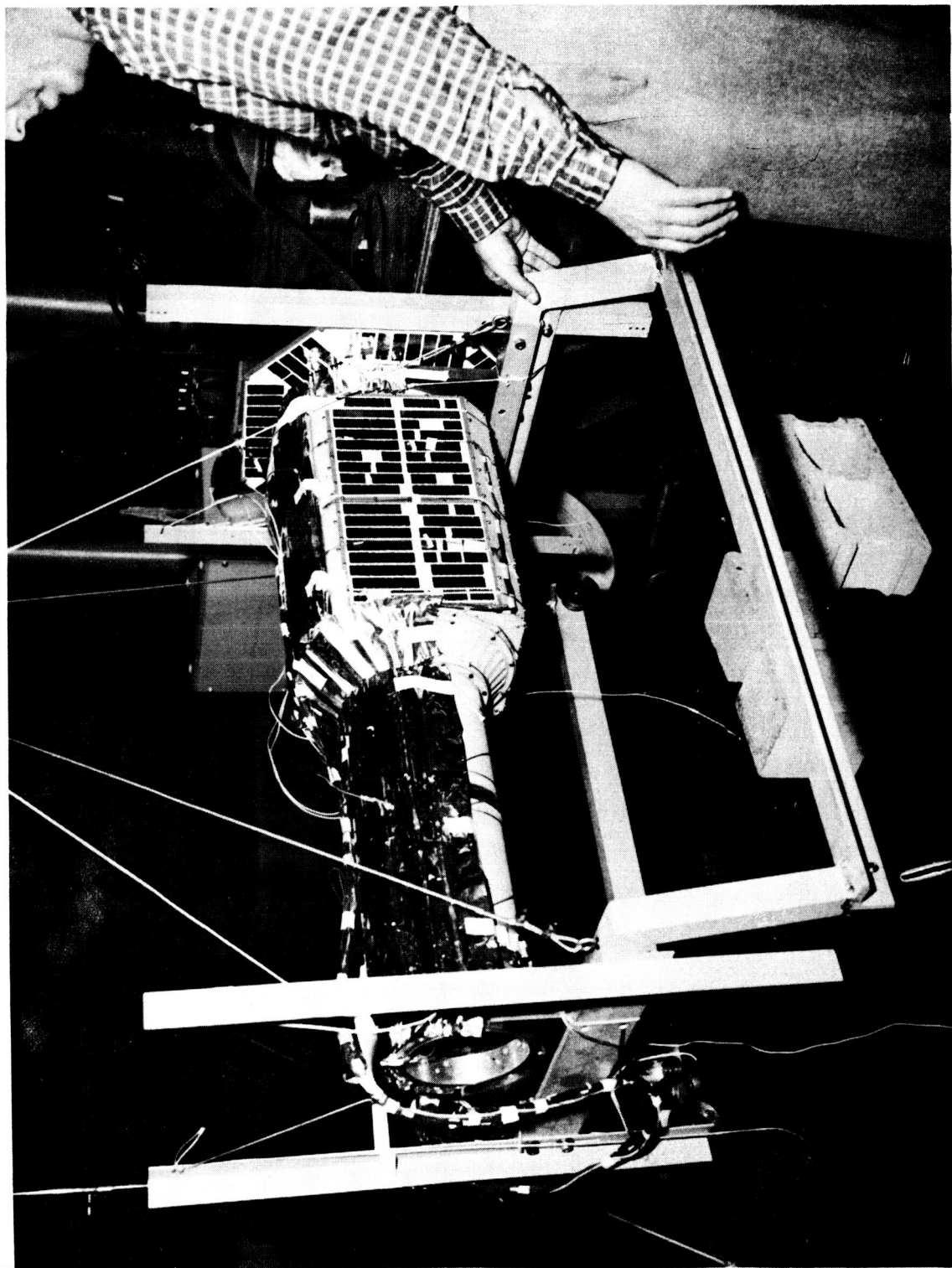


FIGURE 17. HALF-BLANKET ON PROTOTYPE



MTP-RP-61-17

FIGURE 18. HALF-BLANKET COVERED BY FOIL REFLECTOR

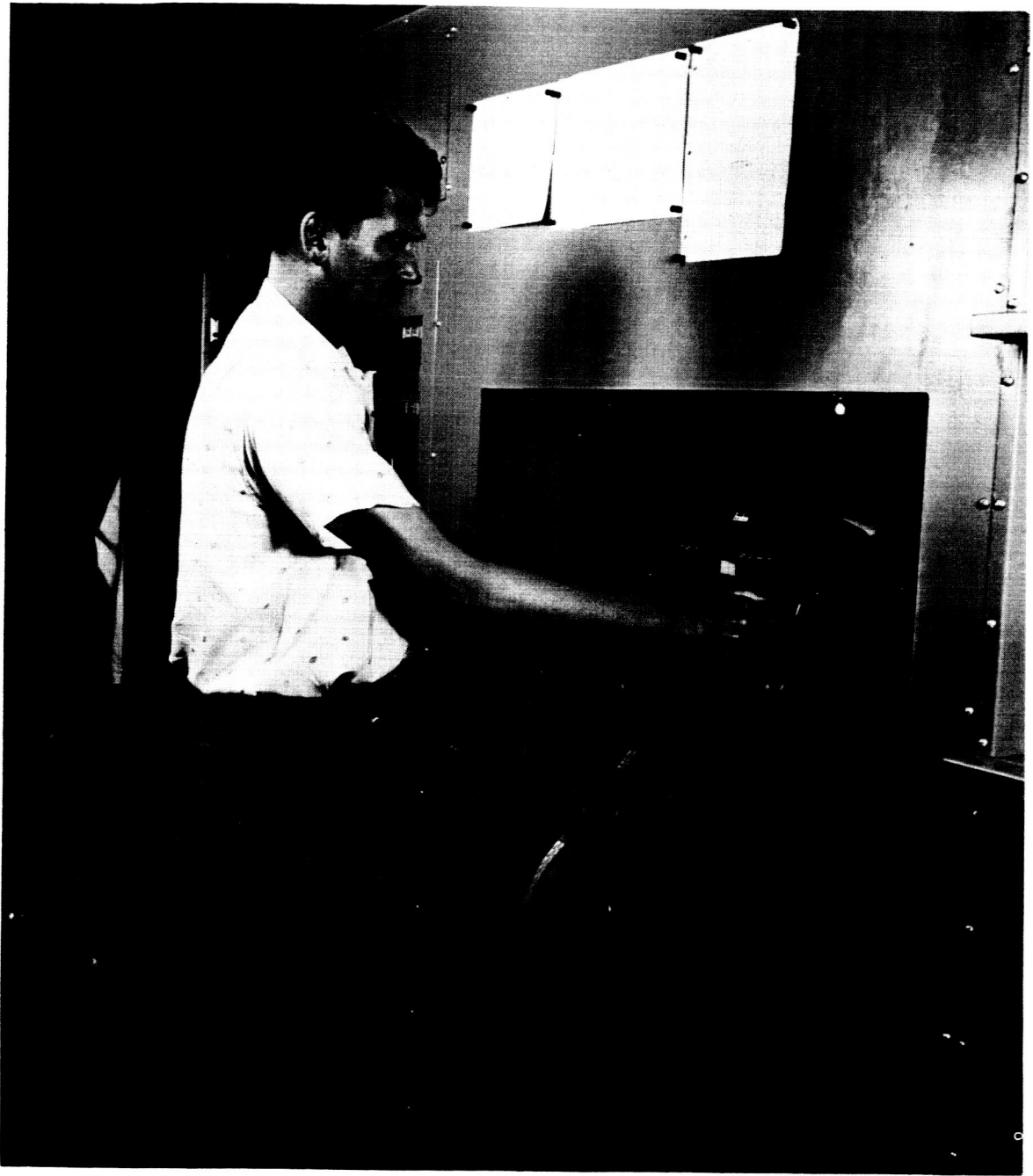
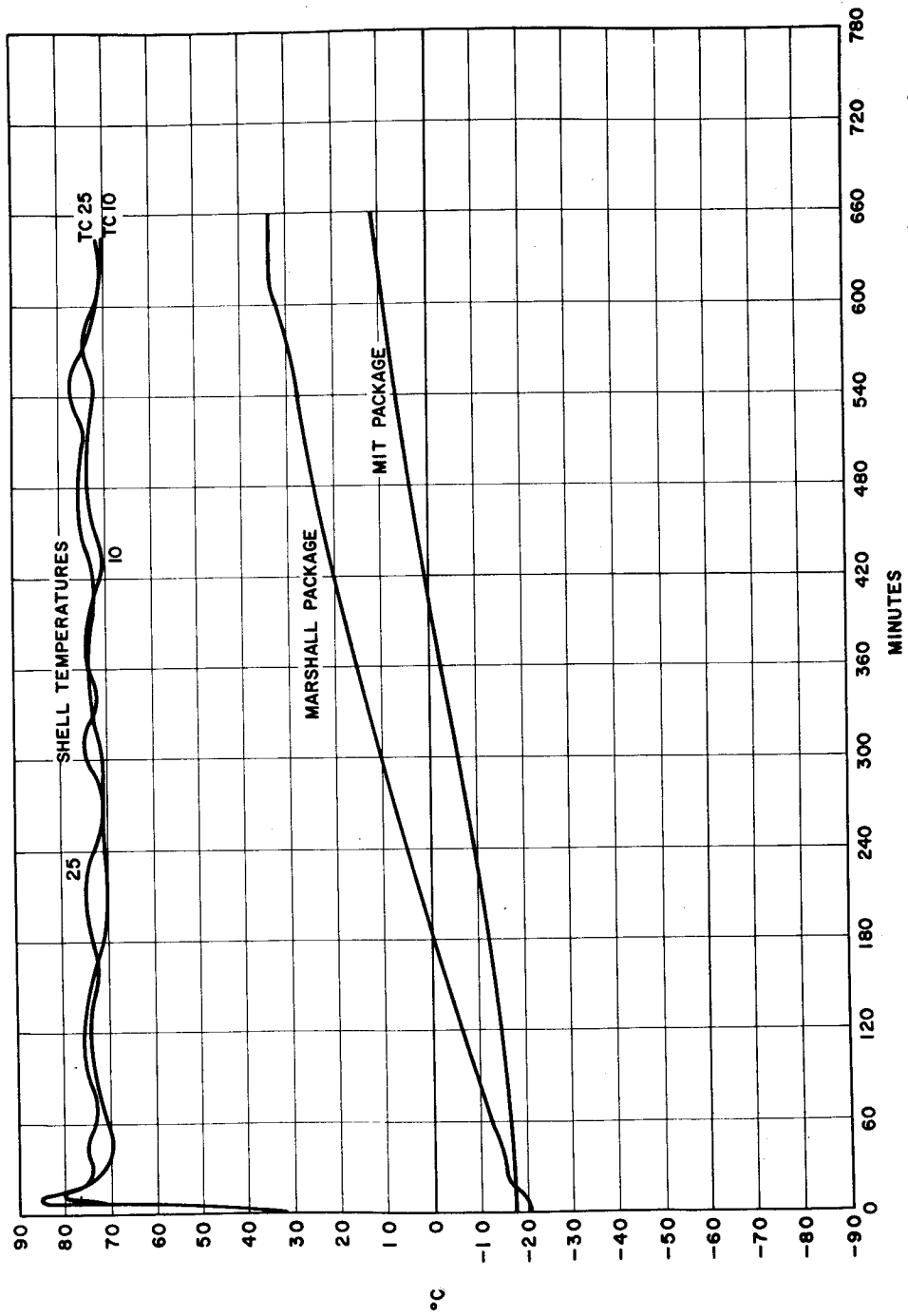


FIGURE 19. DIGITAL DATA RECORDER

MTP-RP-61-17



MTP-RP-61-17

FIGURE 20. RESULTS FROM FULL-BLANKET TEST

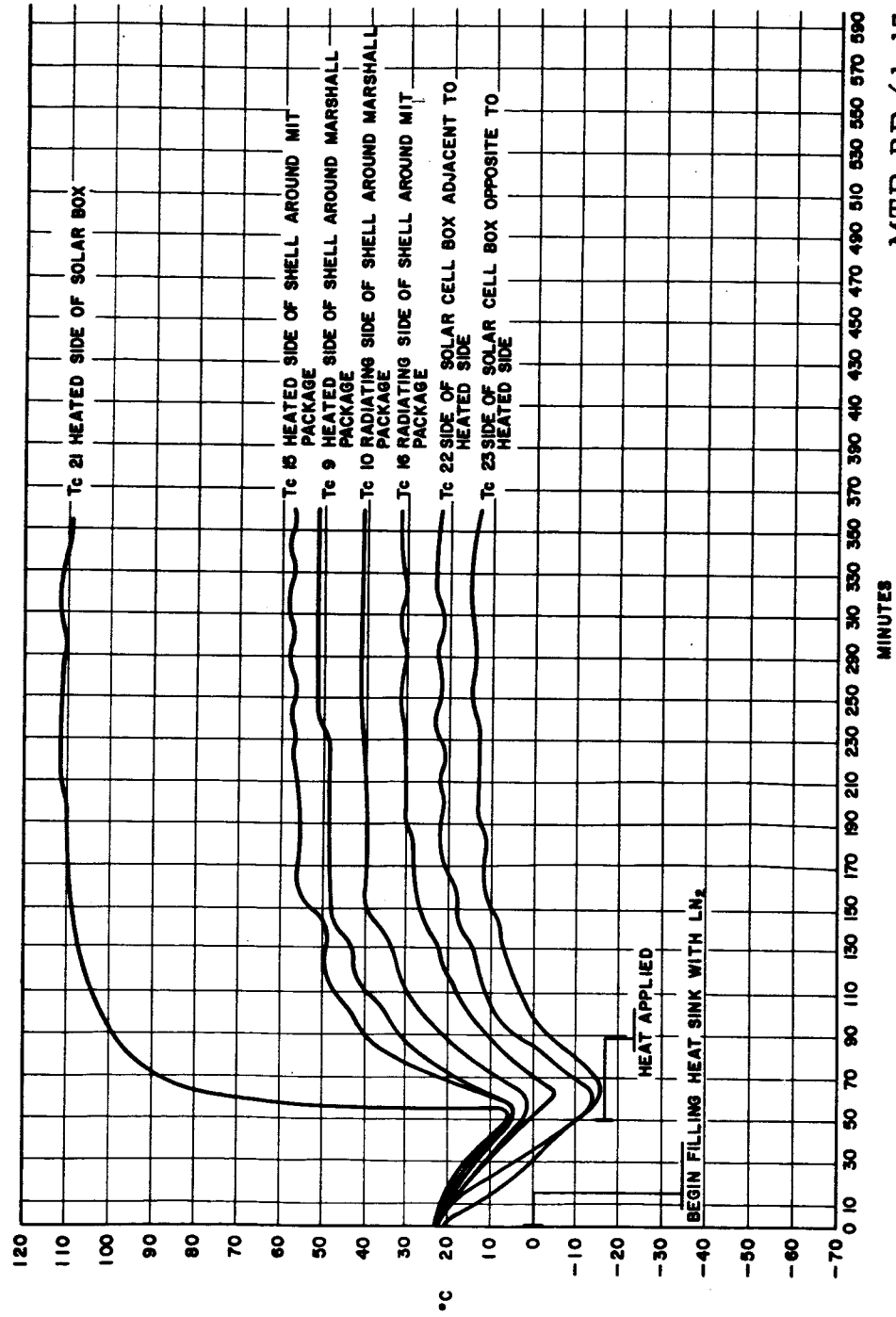


FIGURE 21. RESULTS FROM HALF-BLANKET TEST

SECTION V. RESULTS

The S-15 payload was placed in orbit on April 27, 1961 by the Juno II vehicle, AM-19E (FIG. 22), and was designated Explorer XI, 1961 Nu.

The spin mode of the satellite was expected to change from the original spin about the longitudinal axis to the flat "propeller-like" tumble in a matter of hours or perhaps, at most, a few days. However, this change of mode did not take place until about three weeks after launch. It has been determined that this delay was caused by energy input from the tape recorder (13). At first, it was thought that the mercury in the damper had frozen and rendered it useless for energy dissipation. However, this could not be the case so long as the coatings on the motor case and the damper remained as they were at launch. The temperature of the damper was not monitored, but the temperature of the motor case was, and it can be shown theoretically that for the temperature of the damper to fall below the freezing point of mercury (-38.87°C), the average temperature of the motor case would have to fall below -100°C . As can be seen from the data in FIGURE 23, the average temperature of the motor case did not fall below approximately -50°C , with the minimum value during a revolution being greater than -70°C .

Eight temperature measurements are being made (using thermistors) and telemetered from the satellite. The location of the measurements are: (1), (2), and (3) inside MIT package, (4) inside battery in Marshall package, (5) solar cell patch on solar cell "box", (6) solar cell patch on solar cell disc, (7) special thermally isolated disc, and (8) motor case.

Analysis of the temperature data indicated that the longitudinal axis about which the satellite was spinning was not remaining space-fixed, but precessing at a rate of approximately 10 to 15 degrees a day. If the momentum vector of the satellite had remained space-fixed, the attitude with respect to the sun would have changed at a maximum rate of less than 1° a day (FIG. 24). Temperature measurements indicate that while the satellite was initially almost broadside to the sun, precession occurred which caused the top end of the satellite to move in the direction of the sun. FIGURE 25 shows the average value of the motor case temperature (during the first 15 minutes after the satellite comes out of the earth's shadow) as a function of time after launch. It can be seen that this average value decreases and passes through a minimum on about May 1, 1961. Since the percent of the orbit in sunlight (FIG. 26) and other orbital parameters are fairly constant during this time, it appears that this change in temperature is due to the payload's exposing less of its surface area to the sun. This is further substantiated by the average temperature of the special thermally isolated disc which is mounted on the top end of the satellite.

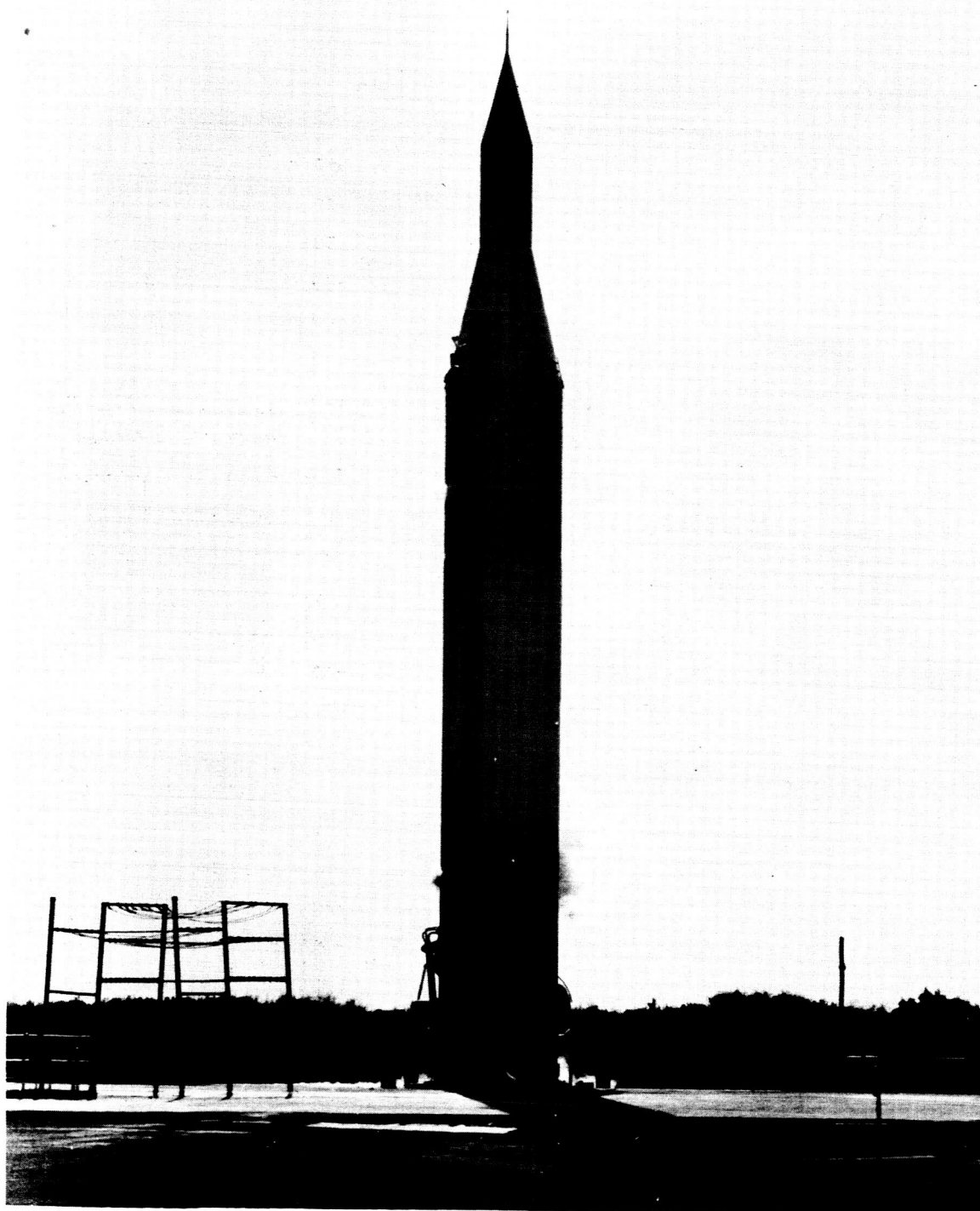
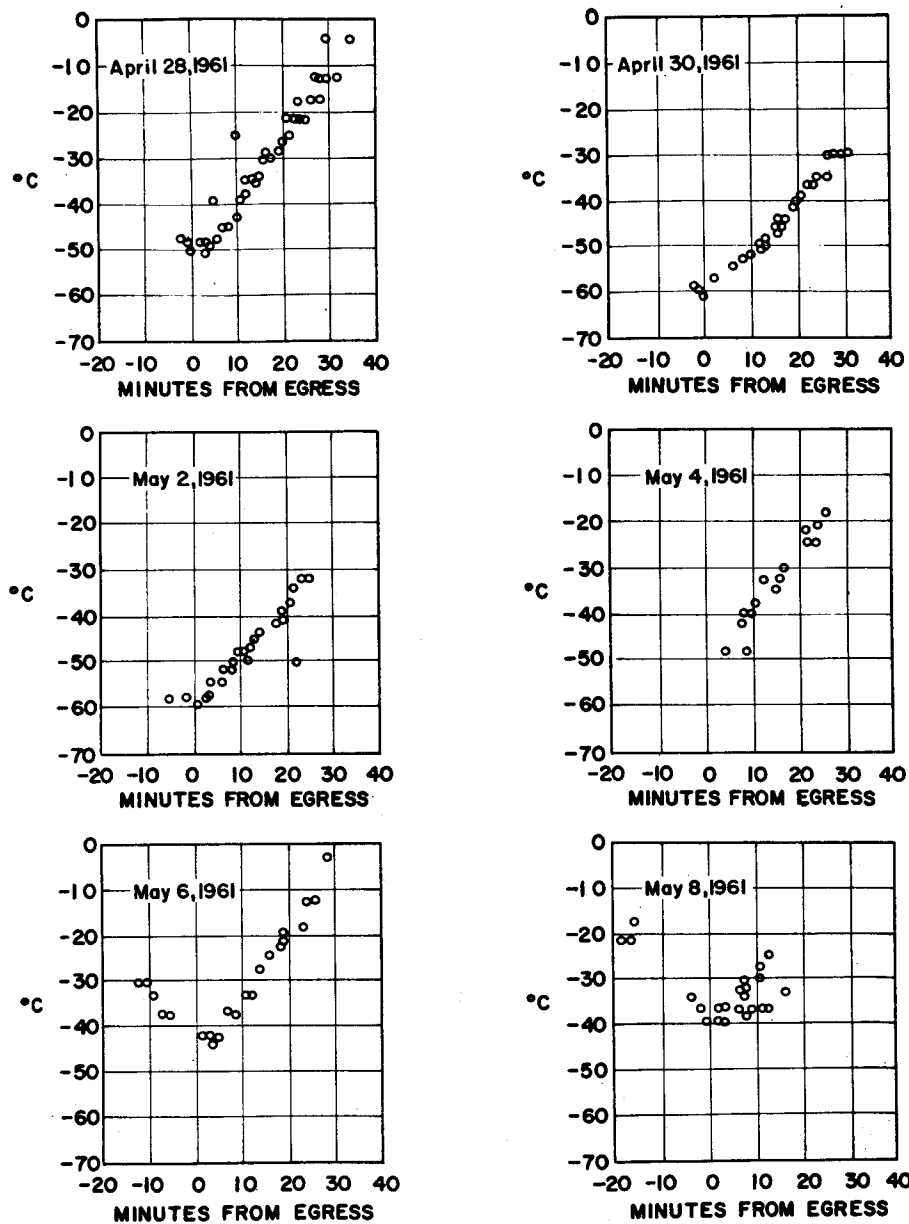


FIGURE 22. JUNO II VEHICLE

MTP-RP-61-17



MTP-RP-61-17

FIGURE 23. TEMPERATURE OF MOTOR CASE VERSUS MINUTES AFTER EGRESS FROM EARTH'S SHADOW

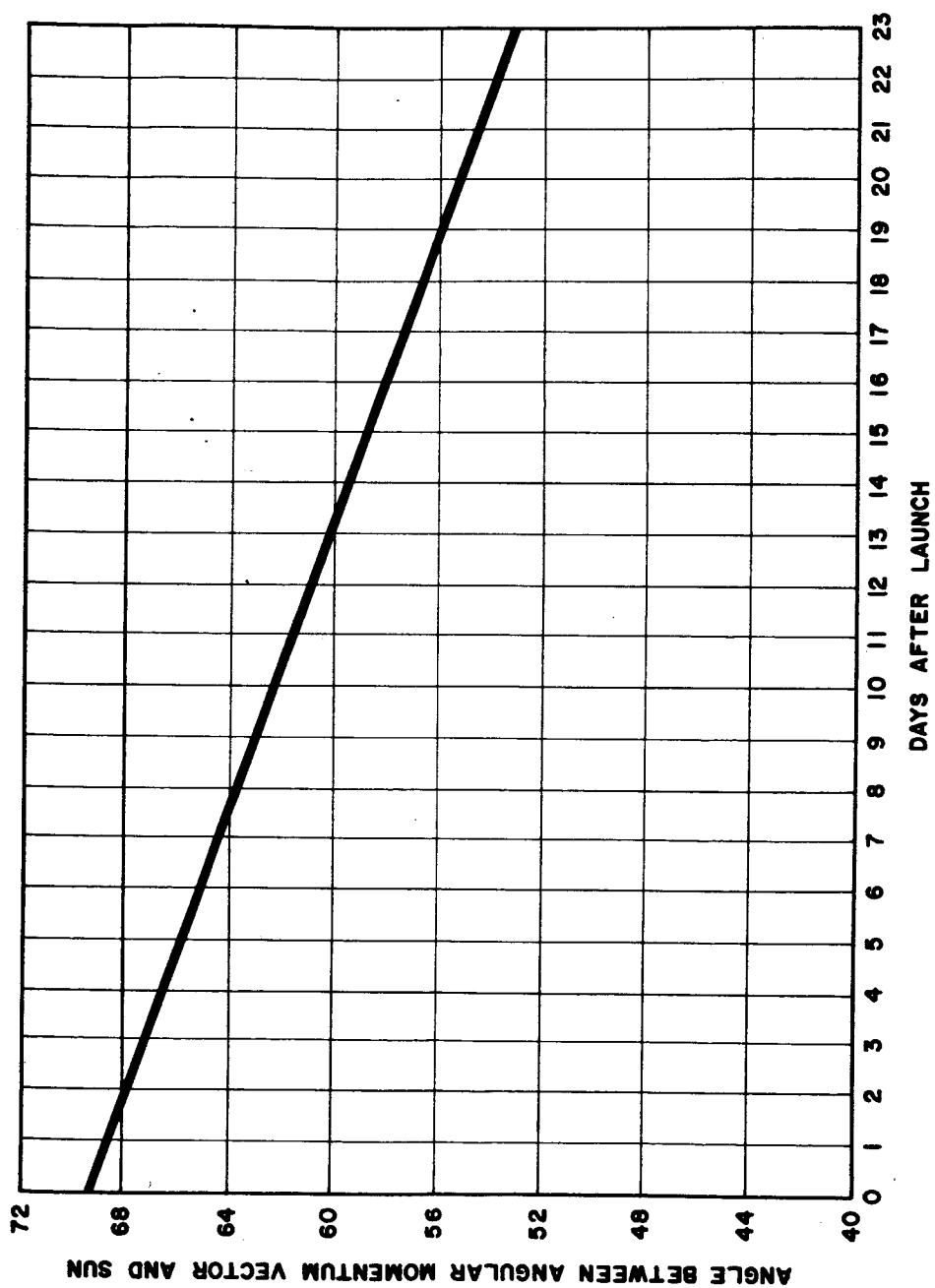


FIGURE 24. THEORETICAL SOLAR ATTITUDE VERSUS DAYS AFTER LAUNCH
MTP-RP-61-17

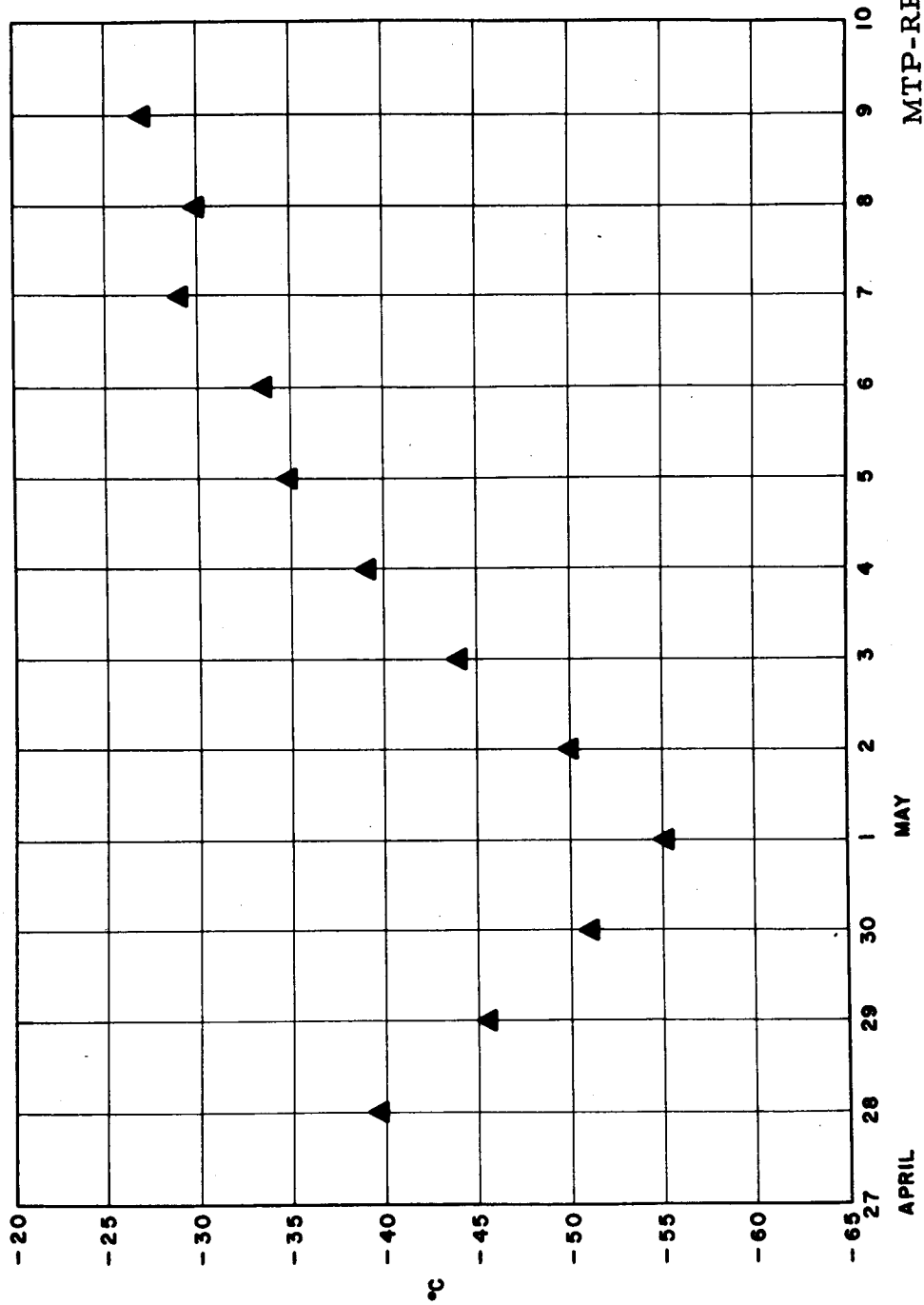
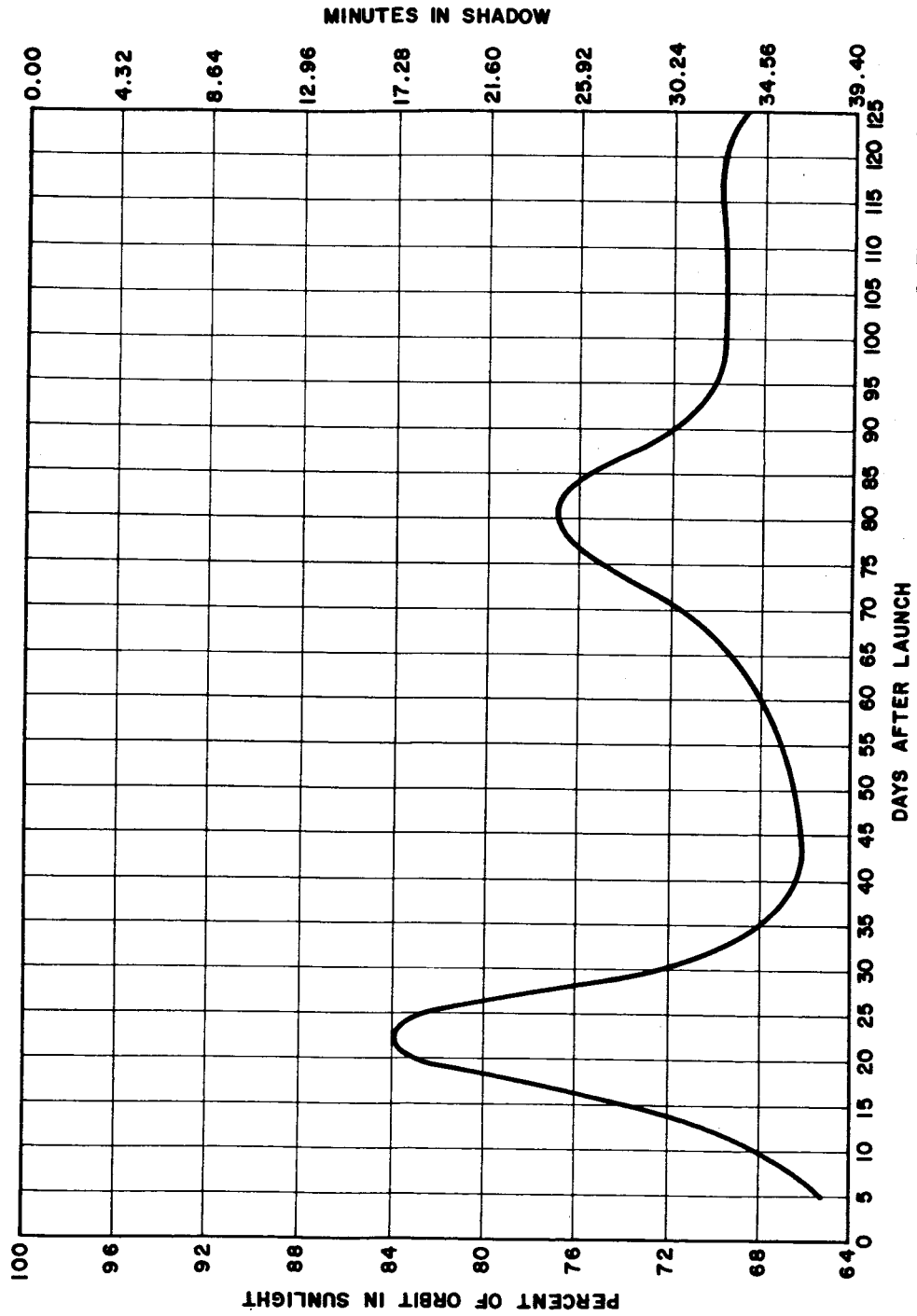


FIGURE 25. AVERAGE VALUE OF MOTOR CASE TEMPERATURE DURING FIRST 15 MINUTES AFTER SATELLITE EMERGES FROM EARTH'S SHADOW VERSUS DAYS AFTER LAUNCH



MTP-RP-61-17

FIGURE 26. PERCENT TIME OF SATELLITE'S ORBIT IN SUNLIGHT

FIGURE 27 shows that the average temperature of the sensor passed through a maximum at the same time the motor case was passing through a minimum. This also indicates that the top end of the payload approached the direction of the sun. The temperature of the solar cell patch on the side of the solar cell "box" and the motor case went through a minimum (FIG. 28) at the same time, while the temperature of the patch on the solar cell disc remained unaffected by the attitude changes. This was due to the increase in solar radiation to the disc as the top end approached the sun, being counterbalanced by a greater heat loss to the colder solar cell box.

The temperatures of the MIT and Marshall packages (FIG. 29) also went through a minimum as the top end of the satellite passed close to the sun. Then, they went through a maximum when the payload was broad-side to the sun and as the percent of the orbit in sunlight increased (FIG. 26).

On the eighteenth day after launch, the shield covering the top end of the MIT package was blown off. This is believed to have been the cause for the rise in temperature of the MIT package which started on that date. At about the same time, the satellite started into a flat tumble (13), and on about the twenty-sixth day after launch, the change in spin mode was completed. From then on the temperature of the sensitive components has remained well within the desired boundaries; the major fluctuations are due to precession of the plane of tumble with respect to the sun. Attitude studies (14) show the temperature fluctuations to be in phase with the fluctuations of the solar aspect angle.

SECTION VI. RESULTS OF SPECIAL TEMPERATURE MEASUREMENTS

There were two special temperature measurements on Explorer XI: one, a measurement on the motor case; the other, a measurement on the thermally isolated disc. Both measurements were of areas which were somewhat thermally isolated from the rest of the satellite. The motor case was isolated by means of the fiberglass antenna gap between it and the payload, Kel-F spacers between it and the antenna can, and fiberglass between it and the mercury damper. The 1 1/2-inch aluminum disc was isolated by mounting it in a special housing (FIG. 30) on top of a Kel-F stem. Both measurements were primarily for the thermal studies of a well defined object in space. The secondary purpose of the measurements was to try to determine the effects of the space environment on a special coating which would be of use in the thermal design of future satellites, probes, and vehicles. The motor case was painted with a white zinc sulfide pigmented air-dry silicone (15) developed and applied by Mr. G. Zerlaut, Structures and Mechanics Division, while the aluminum disc was coated first with a 1 1/2-wavelength thickness of SiO₂; then 200 angstroms of germanium; and finally a 1/4-wavelength thickness of SiO₂ by Dr. G. Hass and Mr. Bradford of the Corps of Engineers, Ft. Belvoir, Virginia.

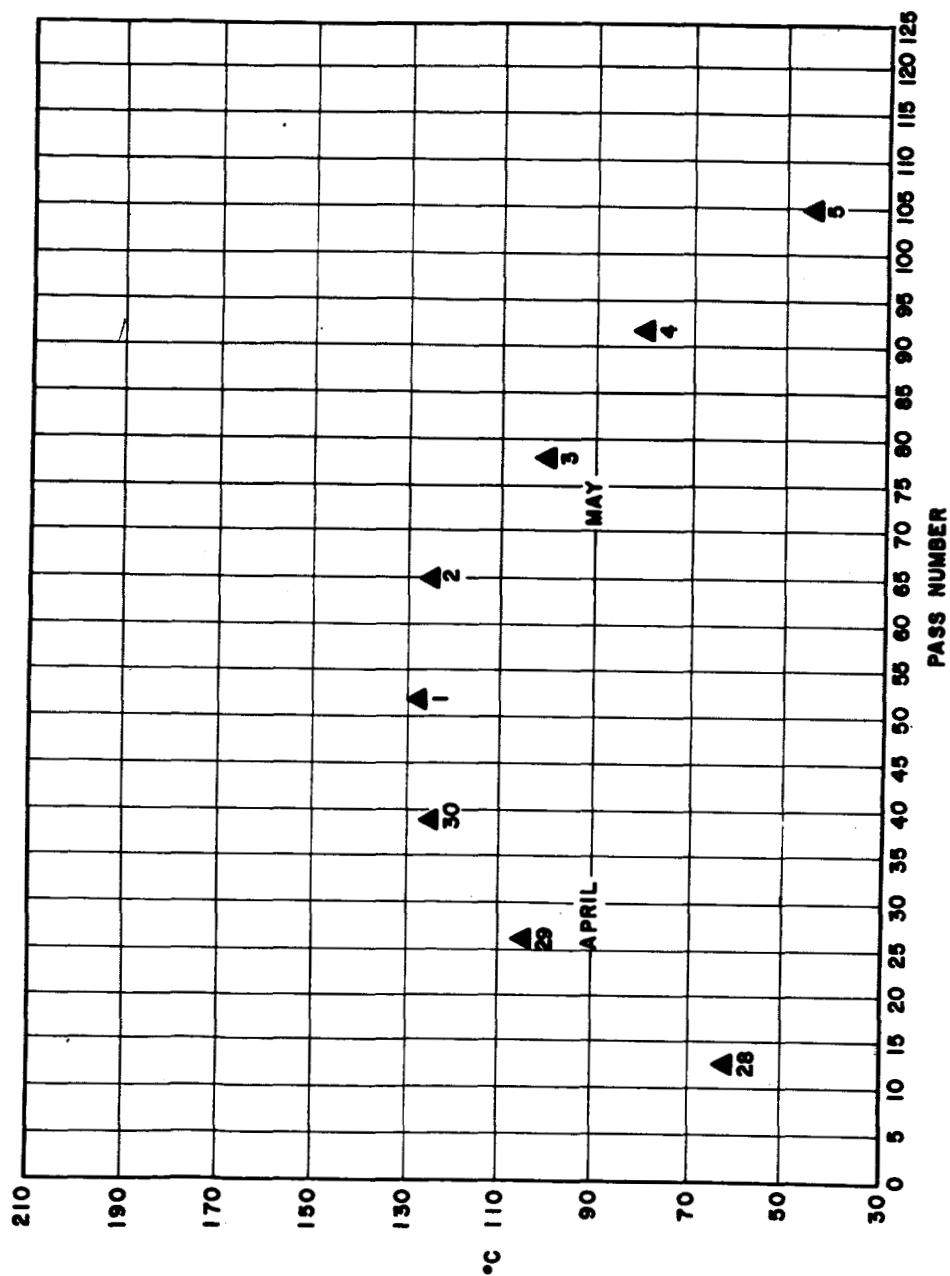


FIGURE 27. TEMPERATURE OF THERMALLY ISOLATED SENSOR VERSUS DAYS AFTER LAUNCH

MTP-RP-61-17

MTP-RP-61-17

FIGURE 28. TEMPERATURE OF SOLAR CELL PATCHES VERSUS MINUTES FROM EGRESS AND PASS NUMBER

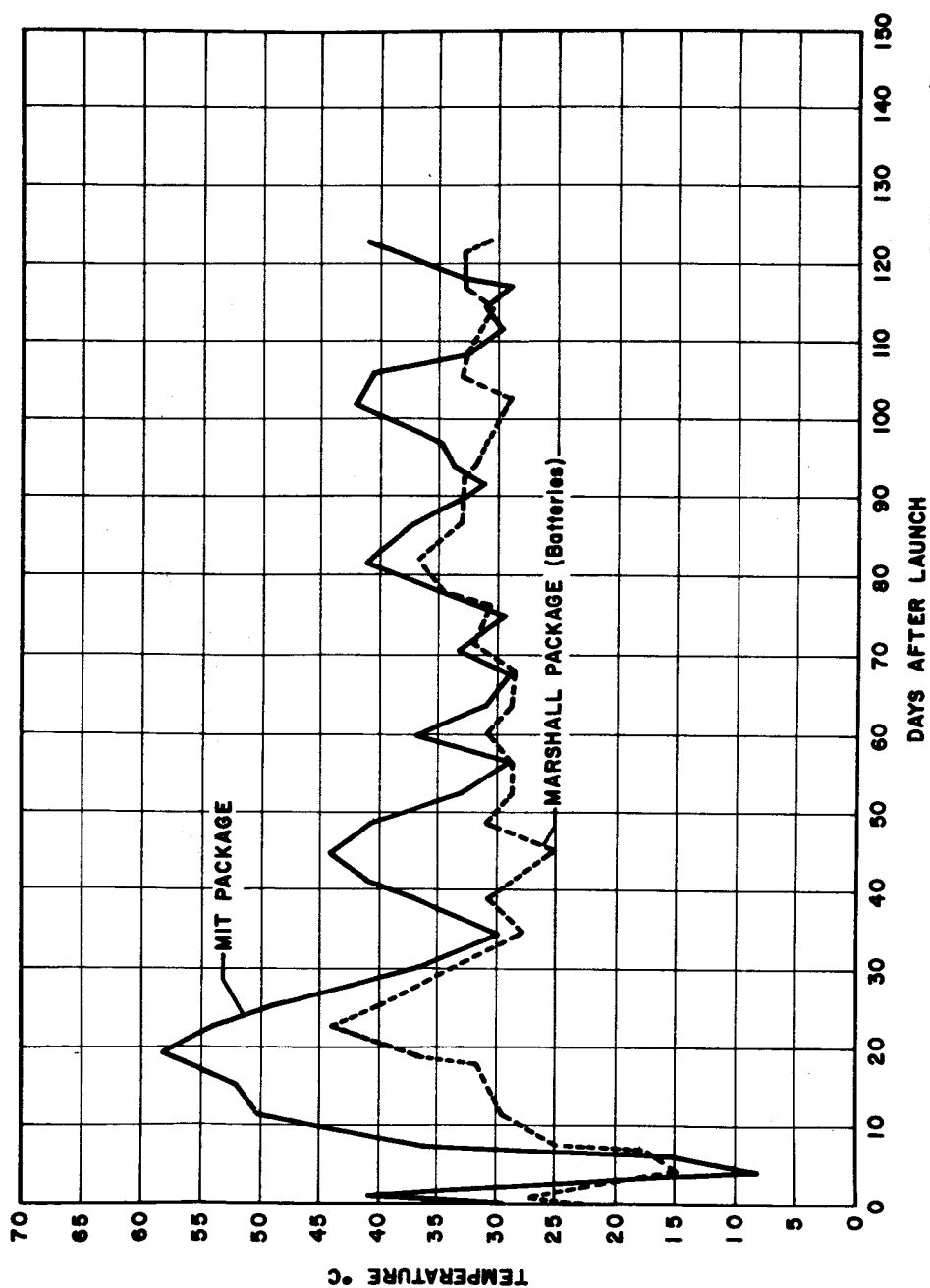


FIGURE 29. TEMPERATURES OF MIT AND MARSHALL PACKAGES VERSUS
DAYS AFTER LAUNCH

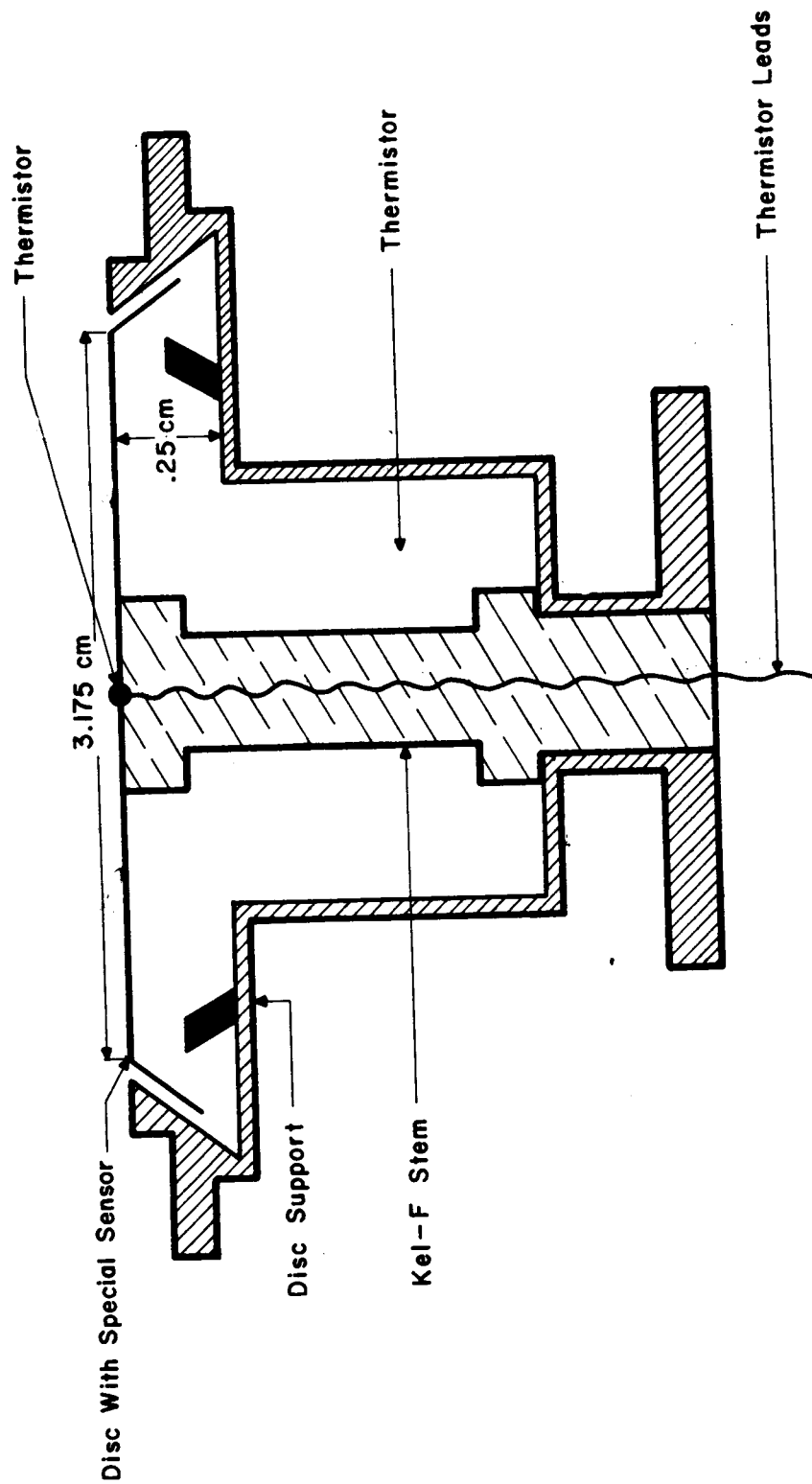
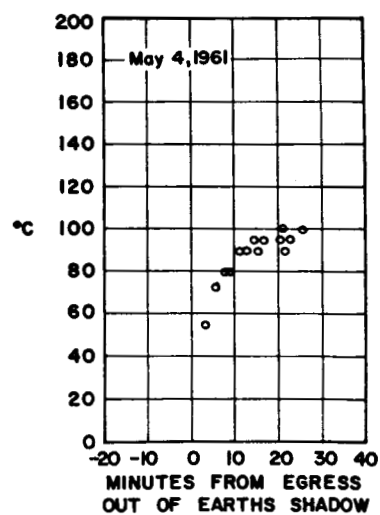
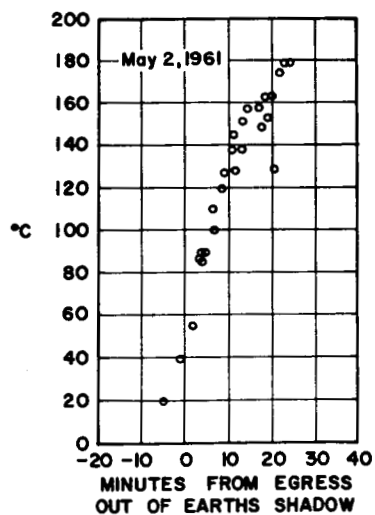
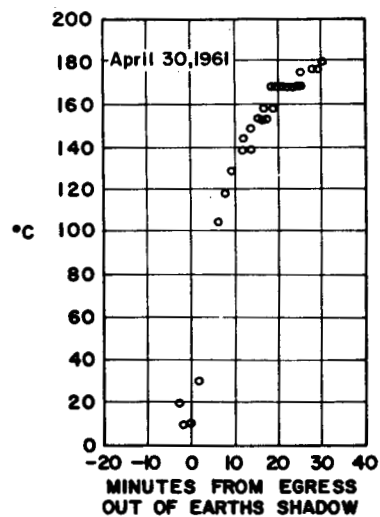
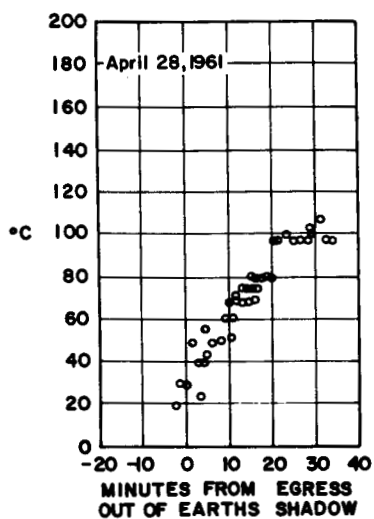


FIGURE 30. THERMALLY ISOLATED TEMPERATURE SENSOR

MTP-RP-61-17

As was expected, the white paint on the motor case caused the temperature to run low (FIG. 23). A detailed analysis of the data has been hampered by lack of accurate solar aspect data during the first two weeks in orbit. During the later period, when the aspect angles are known, strong temperature gradients around the motor case caused by the longitudinal spin reducing to zero make the analysis of the thermal data difficult. It is felt that additional work will make possible definite conclusions concerning the effects of the space environment on the paint.

The coating on the thermally isolated aluminum disc has a solar absorptivity to infrared emissivity ratio of 6.6 (8) which caused the temperature of the disc to run high (FIG. 31). The major block in the analysis of this data was the lack of knowledge of just how thermally isolated the thermally isolated disc is. Measurements have been made (16) and the results will soon be incorporated into the analysis of these data.



MTP-RP-61-17

FIGURE 31. TEMPERATURE OF THERMALLY ISOLATED TEMPERATURE SENSOR VERSUS MINUTES AFTER EGRESS FROM EARTH'S SHADOW

REFERENCES

1. Revised Description and Performance Requirements for NASA Project S-15, Gamma Ray Astronomy Satellite - Juno II (19-e) October, 1959.
2. Ledford, H. & Rankin, T.: Actual Trajectory for Juno II Test Flight AM-19E (U), Marshall Rpt. No. MTP-AERO-61-50, June, 1961.
3. Kuebler, Manfred E.: Gyroscopic Motion of an Unsymmetrical Satellite under no External Force, NASA Rpt. TN-D-596, December, 1960.
4. Naumann, R.: Attitude Determination of Explorer IV, ABMA Rpt. DV-TN-19-59, June, 1959.
5. Heller, G.: The Temperature of an Orbiter, ABMA Rpt. DV-TN-44, June, 1957.
6. Heller, G.: Temperature Problems of the Satellite Missile, ABMA Rpt. DV-TN-62-58, January 1958.
7. Heller, G.: Thermal Problems of Satellites, ABMA Rpt. DV-TN-73-58, September, 1958.
8. Snoddy, W. C.: Thermal Design and Testing of S-46, ABMA Rpt. DV-TM-15-60, June, 1960.
9. Snoddy, W. C.: Temperature Control of the S-30 Payload (Explorer VIII), Marshall Rpt. MTP-RP-61-14, August, 1961.
10. Snoddy, W. C.: Temperature Control of the S-45 Payload, Marshall Rpt. MTP-RP-61-16, September, 1961.
11. Merrill, R. B.: Theoretical Temperature Program on IBM 7090 for S-15 Payload (19-e), Marshall Internal Paper, September, 1961.
12. Jones, B. P.: Thermal Design Test of the IGY Satellite (Payload of Missile No. 16), ABMA Rpt. No. DV-TM-23-59, August 1959.
13. Kuebler, M. E.: Spin-Tumble Transfer of Satellite S-15 (Explorer XI), Marshall Rpt. Nr. MTP-G&C-61-30, July, 1961.
14. Bobo, B. S.: Solar Aspect Angle Determination, Marshall Internal Paper, August, 1961.

REFERENCES (Cont'd)

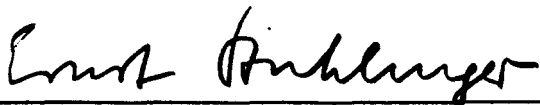
15. Zerlaut, G. A.: Trips to the Launch Operations Directorate, Cape Canaveral, Fla. Memo from M-S&M-MC, April 4, 1961.
16. Lumpkin, C.: Heat Transfer Measurements on the Explorer XI Temperature Sensor, Marshall Internal Note, M-RP-INT-61-21, September, 1961.

APPROVAL

MTP-RP-61-17

TEMPERATURE CONTROL OF THE S-15 PAYLOAD
(EXPLORER XI)

By William C. Snoddy

A handwritten signature in dark ink, reading "Ernst Stuhlinger", is positioned above a horizontal line.

ERNST STUHLINGER
Director, Research Projects Division

DISTRIBUTION

M-DIR

Dr. von Braun
Dr. Rees

M-SAT

Dr. Lange
Mr. Cooper (5) NASA Hq.

M-G&C

Dr. Haeussermann
Mr. Boehm
Mr. Pfaff
Mr. Wagner
Mr. Kampmeier
Mr. Brandner
Mr. Noel
Mr. Taylor
Mr. Hoberg
Mr. Fichtner
Mr. Cagle
Mr. McLain

M-RP

Dr. Stuhlinger
Mr. Heller
Dr. Lundquist
Dr. Shelton
Dr. Schocken
Mr. Thompson
Mr. Bucher
Mr. Miles
Mr. Snoddy (5)
Mr. Jones
Mr. Cochran (2)
Mr. Bulette
Mr. Gates
Mr. Atkins
Mr. Fountain
Reserve (25)

M-COMP

Dr. Hoelzer

M-F&AE

Mr. Nowak

M-AERO

Dr. Geissler

M-QUAL

Mr. Grau

M-TEST

Mr. Heimbarg

M-S&M

Mr. Mrazek
Mr. Zerlaut

M-MS-IPL (8)

M-MS-IP

M-MS-H

M-PAT

Mr. John Warden